frontiers | Frontiers in Cellular and Infection Microbiology

TYPE Original Research
PUBLISHED 21 November 2022
DOI 10.3389/fcimb.2022.1037387

OPEN ACCESS

EDITED BY
Job E. Lopez,
Baylor College of Medicine,
United States

REVIEWED BY
Justin A. Thornton,
Mississippi State University,
United States
Jan Perner,
Biology Centre of the Czech Academy of Sciences, Czechia
Artem Rogovskyy,
Texas A&M University, United States

*CORRESPONDENCE
Shahid Karim
Shahid.Karim@usm.edu

SPECIALTY SECTION
This article was submitted to Parasite and Host, a section of the journal Frontiers in Cellular and Infection Microbiology

RECEIVED 05 September 2022
ACCEPTED 03 November 2022
PUBLISHED 21 November 2022

CITATION
Adegoke A, Kumar D, Budachetri K and Karim S (2022) Hematophagy and tick-borne Rickettsial pathogen shape the microbial community structure and predicted functions within the tick vector, *Amblyomma maculatum*. *Front. Cell. Infect. Microbiol.* 12:1037387.
doi: 10.3389/fcimb.2022.1037387

Hematophagy and tick-borne Rickettsial pathogen shape the microbial community structure and predicted functions within the tick vector, *Amblyomma maculatum*

Abdulsalam Adegoke[1], Deepak Kumar[1], Khemraj Budachetri[1,2] and Shahid Karim[1,3]*

[1]School of Biological, Environmental, and Earth Sciences, University of Southern Mississippi, Hattiesburg, MS, United States, [2]Department of Veterinary Biosciences, The Ohio State University, Columbus, OH, United States, [3]Center for Molecular and Cellular Biosciences, University of Southern Mississippi, Hattiesburg, MS, United States

Background: Ticks are the primary vectors of emerging and resurging pathogens of public health significance worldwide. Analyzing tick bacterial composition, diversity, and functionality across developmental stages and tissues is crucial for designing new strategies to control ticks and prevent tick-borne diseases.

Materials and methods: Here, we explored the microbial communities across the developmental timeline and in different tissues of the Gulf-Coast ticks (*Amblyomma maculatum*). Using a high-throughput sequencing approach, the influence of blood meal and *Rickettsia parkeri*, a spotted fever group rickettsiae infection in driving changes in microbiome composition, diversity, and functionality was determined.

Results: This study shows that the core microbiome of *Am. maculatum* comprises ten core bacterial genera. The genus *Rickettsia, Francisella*, and *Candidatus_Midichloria* are the key players, with positive interactions within each developmental stage and adult tick organ tested. Blood meal and *Rickettsia parkeri* led to an increase in the bacterial abundance in the tissues. According to functional analysis, the increase in bacterial numbers is positively correlated to highly abundant energy metabolism orthologs with blood meal. Correlation analysis identified an increase in OTUs identified as *Candidatus Midichloria* and a subsequent decrease in *Francisella* OTUs in *Rickettsia parkeri* infected tick stages and tissues. Results demonstrate the abundance of *Rickettsia* and *Francisella* predominate in the core microbiome of *Am. maculatum*, whereas *Candidatus_Midichloria* and *Cutibacterium* prevalence increase with *R. parkeri-infection*. Network analysis and functional annotation suggest that *R. parkeri* interacts positively with *Candidatus_Midichloria* and negatively with *Francisella*.

10.3389/fcimb.2022.1037387

Conclusion: We conclude that tick-transmitted pathogens, such as *R. parkeri* establishes infection by interacting with the core microbiome of the tick vector.

KEYWORDS

Amblyomma maculatum, Gulf Coast tick, *Rickettsia parkeri*, 16S rRNA, microbiome, endosymbiont, network analysis, ontogeny

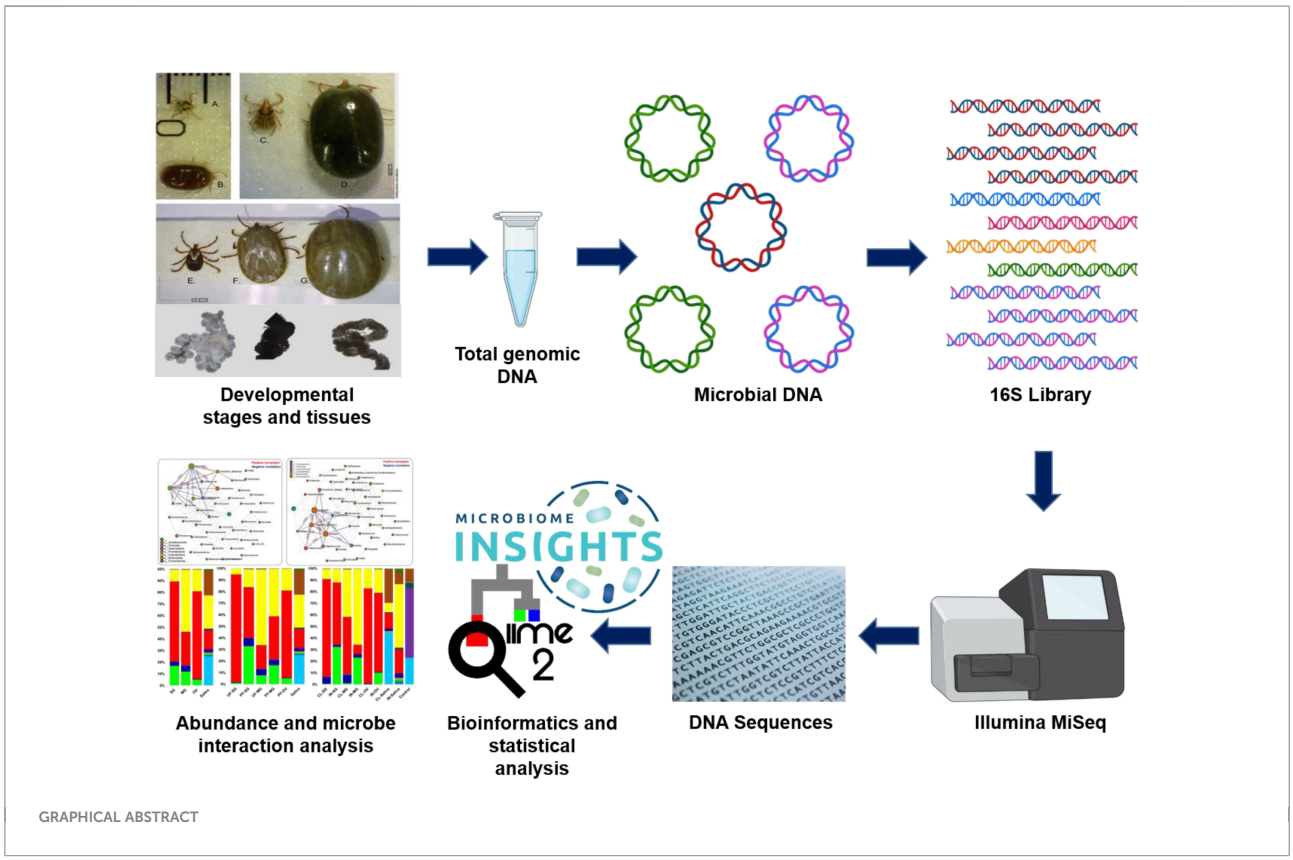

GRAPHICAL ABSTRACT

Introduction

Ticks are obligate hematophagous arthropods that predominantly depend on human and animal host blood for development. Their importance as vectors of human and animal pathogens is highlighted by the substantial resources channeled towards controlling the several tick-transmitted pathogens. The Gulf Coast tick (*Amblyomma maculatum*) is one of the important human-biting ticks in the United States, along with *Amblyomma americanum, Ixodes scapularis*, and *Dermacentor variabilis. Amblyomma maculatum* (*Am. maculatum*) is the most geographically widespread tick species in the southeastern United States (Sonenshine, 2018). It is the competent vector of *Rickettsia parkeri* (*R. parkeri*), a spotted fever group rickettsial (SFGR) pathogen that causes mild infections in the United States (Paddock and Goddard, 2015).

Recent advances in the control of ticks and tick-transmitted pathogens have led to the discovery of microbial communities that co-exist alongside pathogens (Narasimhan and Fikrig, 2015; Bonnet et al., 2017; Wei et al., 2021; Wu-Chuang et al., 2021; Narasimhan et al., 2021). The functional role of the tick microbiome has only been partly clarified by tick research. Overall, the primary focus of tick microbiome research has been on the microbial profiling of field-collected ticks to understand the basic bacterial profiles/communities present. The tick microbiome is a moving target and investigating its dynamics within the tick vector is a continuous effort (Narasimhan and Fikrig, 2015; Bonnet et al., 2017; Greay et al., 2018; Narasimhan et al., 2021). Ticks specialize in an exclusive diet of vertebrate blood and have evolved intimate interactions with beneficial symbionts that provide essential B vitamins and cofactors deficient or not readily accessed in the

blood diet (Adams, 1963; Gottlieb et al., 2015; Hunter et al., 2015; Smith et al., 2015; Bonnet et al., 2017; Duron et al., 2017; Guizzo et al., 2017; Duron et al., 2018; Olivieri et al., 2019; Ben-Yosef et al., 2020). Correlative evidence also suggests that the tick reproductive fitness may benefit from essential nutrients provided by tick endosymbionts, though this is yet to be experimentally proven (Zhong et al., 2007). Additionally, it has been discovered that specific microorganisms within the tick and other blood-feeding arthropods perform immunomodulatory roles. These microorganisms prime the immune system of the host to continually produce low quantities of antimicrobial peptides, and either inhibit or promote the multiplication of other microbes (de la Fuente et al., 2017; Budachetri et al., 2018; Fogaça et al., 2021; Boulanger and Wikel, 2021; Bonnet and Pollet, 2021).

Several studies have reported on the structure and microbial composition of field-collected and lab-maintained tick populations (Budachetri et al., 2014; Budachetri et al., 2017; Karim et al., 2017; Ross et al., 2018; Varela-Stokes et al., 2018; Portillo et al., 2019; Thapa et al., 2019a; Zhang et al., 2019; Adegoke et al., 2020; Gil et al., 2020; Guizzo et al., 2020; Kumar et al., 2022; Maldonado-Ruiz et al., 2021; Rojas-Jaimes et al., 2021). These studies have revealed a variety of factors responsible for the differences among microbial communities between different tick samples, thus contributing extensively to our understanding of how microbial communities residing within the tick contribute to several aspects of tick biology (Ponnusamy et al., 2014; Budachetri and Karim, 2015; Trout Fryxell and DeBruyn, 2016; Budachetri et al., 2018; Thapa et al., 2019b; Adegoke et al., 2020; Brinkerhoff et al., 2020; Kueneman et al., 2021). However, the structure of *Am. maculatum* microbial communities and how these communities are shaped by blood meal and pathogen interactions have been the focus of two studies (Budachetri et al., 2014; Budachetri et al., 2018). Previous microbiome studies of *Am. maculatum* identified unique differences in microbial composition and abundance of specific bacterial genera in field-collected and questing tick tissues (Budachetri et al., 2014). The ability of a tick to serve as a competent vector for any pathogen goes beyond the establishment of the pathogen within the tick tissue. It also extends to the facilitation of pathogen transmission at the tick–host interface, which is made possible in part by salivary proteins. This process is described as saliva-assisted transmission (Nuttall and Labuda, 2008; Šimo et al., 2017; Nuttall, 2019; Karim et al., 2021). Whether the tick salivary microbiome interferes or facilitates pathogen colonization and transmission remains an unanswered question. While a study by Budachetri et al. (2014) reported several *Rickettsia* species in the saliva of *Am. maculatum*, only *R. parkeri* was detected in the salivary glands of *Am. maculatum*. Limited information exists about how microbial community members interact across tick developmental stages and tissues and how these tissues shape or modulate microbial community assemblages during tick physiological changes, such as those following blood-feeding or pathogen interactions. An elegant study by Lejal et al. (2021) identified several positive and negative correlations between members of the field-collected, questing *Ixodes ricinus* microbiome and how some of these interactions are modulated by tick-borne pathogens. It has been established that each tick tissue (organ) undergoes unique responses to specific physiological changes, but it is not known whether these responses also induce changes in the microbial communities residing within these tissues (Franta et al., 2010; Schwarz et al., 2014; Crispell et al., 2016; Kumar et al., 2016; Budachetri et al., 2017; Starck et al., 2018; Tirloni et al., 2020; Kurokawa et al., 2020). In the current study, a high-throughput sequencing approach was utilized to examine microbiome changes throughout the ontogeny of uninfected and pathogen-infected *Am. maculatum* ticks. Characterization of unique microbe-microbe interactions (measure of the degree of relationships between genera) at the different tick developmental stages and tissues revealed potential synergistic and antagonistic interactions among the bacterial communities.

Materials and methods

Ethics statement

All animal experiments were conducted in strict accordance with the recommendations of the Guide for the Care and Use of Laboratory Animals of the National Institutes of Health, USA. The protocols for the blood-feeding of immature and mature development stages of *Am. maculatum* were approved by the Institutional Animal Care and Use Committee of the University of Southern Mississippi (protocols #15101501.2 and 15011402).

Tick maintenance

Rickettsia parkeri-infected and uninfected *A. maculatum* ticks were maintained under laboratory conditions as previously described (Budachetri et al., 2014; Budachetri et al., 2017; Budachetri et al., 2018). The colonies were established from field-collected adult ticks collected in 2011 from the Mississippi Sandhill Crane, National Wildlife Refuge (https://www.fws.gov/refuge/mississippi_sandhill_crane/) using the drag-cloth method. To generate replete adult females, unfed male and female *Am. maculatum* ticks were infested on sheep and allowed to feed to repletion and drop off. Fully engorged female ticks were then allowed to oviposit in individual snap-cap vials with perforated lids protected by breathable mesh cloths to allow for oxygen exchange while preventing their escape. Unfed larvae that emerged from the eggs were infested on golden Syrian hamsters until fully engorged, which were then allowed to molt into nymphs and then reinfested on golden Syrian hamsters. The

fully fed nymphs were subsequently allowed to molt into adult male and female ticks. The presence or absence of *R. parkeri* at each developmental stage was confirmed following previously established nested PCR, qPCR and immunofluorescence. Clutches of eggs from ovipositioning females were tested for *R. parkeri* infection and infected females were separated from uninfected female (Budachetri et al., 2014; Budachetri et al., 2018; Guizzo et al., 2022).

Tick life stages and DNA extraction

DNA was isolated from freshly laid eggs as well as unfed and partially fed ticks at various developmental stages: nymphs, male and female adults. To remove surface contaminants and bacterial carryover, all samples from developmental stages were surface-sterilized using 2% sodium hypochlorite, followed by two 5-minute washes in 70% ethanol and two 5-minute washes in sterile deionized water (Kumar et al., 2022). Tissues were dissected from unfed and partially blood-fed adult females and directly stored in tissue lysis ATL buffer (contains sodium dodecyl sulphate as active component) before extracting DNA. Female ticks were used for tissue collection because of their ability to effectively take a blood meal and increase their size throughout the host attachment period compared to males that take minimal blood meal and shows no physical changes. Tick dissection was performed in a biosafety cabinet while changing blades (Personna American Safety Razor, Mexico) between dissections. Saliva was collected on ice by endogenous induction of salivation following injection of pilocarpine, as previously described (Ribeiro et al., 2004; Valenzuela et al., 2000). DNA was extracted using the DNeasy Blood and Tissue Kit following the manufacturer's protocol (QIAGEN, Germantown, MD, USA) in a biosafety cabinet to eliminate potential carryover of bacteria between samples. Control samples included a blank control and a mock bacterial sample with a known bacterial population (ZymoBIOMICS™ Microbial Community DNA Standard, Zymo Research, Irvine, CA, USA) as part of the DNA-extraction protocol.

Library preparation for Illumina 16S sequencing

Library preparation and indexing were carried out according to Illumina 16S metagenomic sequencing. The V3–V4 region of the 16S rRNA gene was amplified using DNA samples from different life stages and tissues. A two-step PCR amplification was carried out, which included an initial V3–V4 amplification using primers with specific Illumina adapter overhang nucleotide sequences using the following thermocycling conditions: 95°C for 3 min; followed by 25 cycles of 95°C for 30 s, 55°C for 30 s, and 72°C for 30 s; and a final extension step of 72°C for 5 min. The PCR amplicon was purified using AmPure XP beads (Agencourt Bioscience Corporation, Beverly, MA, USA) following the manufacturer's protocol, and the purified product was eluted in 50 µl of TE buffer (Qiagen cat. no. 19086, Qiagen, Germantown, MD, USA) and analyzed on a 2% gel to confirm a single DNA band with an estimated amplicon size of 550 bp. The second step involved attaching unique indexes, in the form of nucleotide sequences, to the purified V3–V4 PCR product. Commercially available dual indexes (i5 and i7) from the Illumina Nextera index kit V2 (Illumina, San Diego, CA) were used for the second (index) PCR. Briefly, a reaction including each of the forward and reverse Nextera index primers, high fidelity 1X KAPA HiFi HotStart ReadyMix (Kapa Biosystems, Wilmington, MA, USA), and 5 µl of each purified V3–V4 amplicon was set up using the following thermocycling conditions: 95°C for 3 min; followed by 8 cycles of 95°C for 30 s, 55°C for 30 s, and 72°C for 30 s; and a final extension step of 72°C for 5 min. The PCR product was briefly purified using AmPure XP beads (Agencourt Bioscience Corporation, Beverly, MA, USA), following the manufacturers protocol. The purified product was eluted in 25 µl of TE buffer and analyzed on a 2% gel to confirm a single DNA band with an estimated amplicon size of 630bp. The purified indexed PCR library products were quantified using the KAPA Library Quantification Kit from Roche (cat. no. 07960255001, kit code KK4844, Hoffmann-La Roche, Basel, Switzerland), normalized to a concentration of 7 nM, and pooled with 5 µl of each normalized library. Biological replicates from DNA extraction controls, TE buffer, and mock bacterial communities (ZymoBIOMICS™ Microbial Community DNA Standard, Zymo Research, Irvine, CA, USA) were simultaneously processed alongside the tick samples. The purified library was sequenced in a single run of an Illumina MiSeq sequencing instrument using reagent kit v2 (500 cycles) with 2 X 250 bp output at the University of Mississippi Medical Centre (UMMC) Genomics Core Facility.

Data processing and analysis

Unless otherwise stated, all preprocessing was performed following the video tutorial of the Quantitative Insights into Microbial Ecology (QIIME2) pipeline (Bolyen et al., 2019). Briefly, demultiplexed fastq files were unzipped using the "unzip -q casava-18paired-end-demultiplexed.zip" command, followed by merging individual forward and reverse fastq files into a single fastq file. The Atacama soil microbiome pipeline was incorporated to control demultiplexed paired-end reads using the DADA2 plugin as previously described (Callahan et al., 2016). Low-quality sequences were trimmed and filtered out, and subsequent merging of paired-end reads ensured 20 nucleotide overhangs between forward and reverse reads. Chimeric sequences were removed from the sequence table.

The qiime2 feature-classifier plugin v. 7.0 was used for taxonomic assignment against the pre-trained Silva_132_99% classifier (Quast et al., 2013). The "qiime diversity core-metrics-phylogenetic" command was used to compute diversity metrics, after which the "QIIME diversity alpha-group-significance" command was used to explore microbial diversity using Faith_pd and evenness metrics as measures of community richness and evenness, respectively. To determine the taxa that significantly differ between groups, we used differential abundance analysis (DAA) with the OTU table (at genera-level, taxon = Genus) as input data. *Post-hoc* test (the false discovery rate, FDR) was used to determine significantly different (FDR p-value < 0.05) taxa between groups. Raw sequences were submitted to DRYAD repository (https://doi.org/10.5061/dryad.r2280gbgg).

Functional characterization of microbial communities

To determine the functionality of the microbial genome, we predicted the functional pathways using the Phylogenetic Investigation of Communities by Reconstruction of Unobserved States 2 (PICRUSt2) pipeline (Ye and Doak, 2009; Mirarab et al., 2012; Louca and Doebeli, 2018; Czech et al., 2020; Douglas et al., 2020). We assigned functional predictions by normalizing the bacterial sequences and OTUs to the KEGG Ortholog (KO) databases and Clusters of Orthologous Groups (COGs) to predict metabolic pathways.

Visualization

Microbiome Analyst, a web-based interface, was used for data visualization using taxonomy and metadata tables generated from data processing as input files (Dhariwal et al., 2017; Chong et al., 2020). Low count and prevalence data were filtered from the OTU table by setting values of 10 and 20, respectively. A filtered abundance table was exported and used in generating histograms of bacterial abundance in Microsoft Excel 2016 (Microsoft, 2018). Boxplots of alpha diversity were generated with GraphPad Prism version 8 for Windows (GraphPad Software, La Jolla CA, USA, www.graphpad.com) using the pairwise table generated from the "qiime diversity alpha-group-significance" command. Network correlation maps were constructed based on the sparse correlations for compositional data (SparCC) approach (Friedman and Alm, 2012). This approach uses the log-transformed values to carry out multiple iterations, which subsequently identifies taxa outliers to the correlation parameters (Chong et al., 2020). To compare the differences in the microbiome between tick groups based on measures of distance or dissimilarity, a matrix was generated from log-transformed sequence data, and ordination of the plots was visualized using both Principal Coordinates Analysis (PCoA) and non-metric multidimensional scaling (NMDS). The Bray–Curtis distance matrix was used to visualize compositional differences in the microbiome across all groups.

Statistical analysis

The Wilcoxon rank-sum test estimated significant correlations in diversity indexes across developmental stages and tissue data sets. A Kruskal–Wallis test followed by Dunn's multiple comparison test was used in comparing the effect of blood meal and *R. parkeri* on microbial richness between two different groups (unfed vs. fed or uninfected vs. infected). Statistically significant data were represented as $P < 0.05$.

Results

Sequencing results

A total of 91 samples, representing at least three biological replicates across developmental stage (egg, larvae, nymph, and adult), tissue (salivary gland, midgut, and ovary), and body fluids (saliva) from uninfected and *R. parkeri*-infected ticks, generated a total of 4,090,811 forward and reverse reads, with a mean of 45,453.5 and a maximum of 112,242 reads per sample (Additional File, Table S1). Rarefaction analysis of the individual samples from a sequencing depth of 500 to 4000 confirmed that there was adequate sequence coverage relative to the number of operational taxonomic units (OTUs) and a plateau for individual tick samples (Additional File, Figures S1A, B). Overall, 711 unique OTUs were identified, with 254 identified from each developmental stage and tissue.

Microbiome dynamics across developmental stages

Proteobacteria represented the most abundant phylum throughout ontogeny, with a relative abundance of 84%, followed by Actinobacteria, Firmicutes, and an uncharacterized phylum (Additional File, Figure S2A). An extended breakdown of each identified phylum and the number of member bacteria at the genus level is represented using pie charts for each phylum, as shown in Additional File, Figures S2B–D. The breakdown of the top 10 most frequent bacterial genera shows that *Francisella* and *Rickettsia* were the predominant members of the *Am. maculatum* microbiome across all developmental stages (Additional File, Figure S3A).

We observed a progressive decrease in the relative abundance of the genus *Cutibacterium* throughout each developmental stage, from egg to adult male and female ticks (Additional File, Figure S3A). Other bacterial genera, such as *Rhodococcus*, *Pseudomonas*, and *Candidatus_Midichloria*, were also detected at relatively lower abundance. The abundance of representative bacterial genera was also compared between blood-fed and unfed life stages. Uptake of a blood meal was observed to impact the relative abundance of *Francisella* and *Cutibacterium* (Additional File, Figure S3B). Fed larvae showed a decrease in *Francisella* abundance and an increase in the abundance of *Cutibacterium* compared to unfed larvae.

Interestingly, opposing trends were observed when blood-fed nymphs were compared with unfed nymphal ticks. The relative abundance of *Cutibacterium* was reduced, whereas *Francisella* abundance was observed to increase (Additional File, Figure S3B). To examine the modulation of microbial assemblages in the presence of pathogenic microbes, we compared the relative abundances of bacteria between uninfected and *R. parkeri*-infected samples from each developmental stage. There is a clear trend of decreasing *Francisella* abundance, and the corresponding increase in *Rickettsia* and *Candidatus_Midichloria* across all *R. parkeri*-infected stages compared with uninfected samples (Additional File, Figure S3C). Notably, the *Cutibacterium* load was negatively impacted by the presence of *R. parkeri* when infected and uninfected nymphs were compared (Additional File, Figure S3C).

Eggs exhibited higher bacterial richness and evenness, regardless of blood meal or infection (Wilcoxon rank-sum test $p < 0.05$). At the same time, nymphs showed the least microbial richness and evenness (Wilcoxon rank-sum test $p < 0.001$) (Figures 1A, B). No significant microbial richness in the blood-fed samples was observed; however, blood meal was

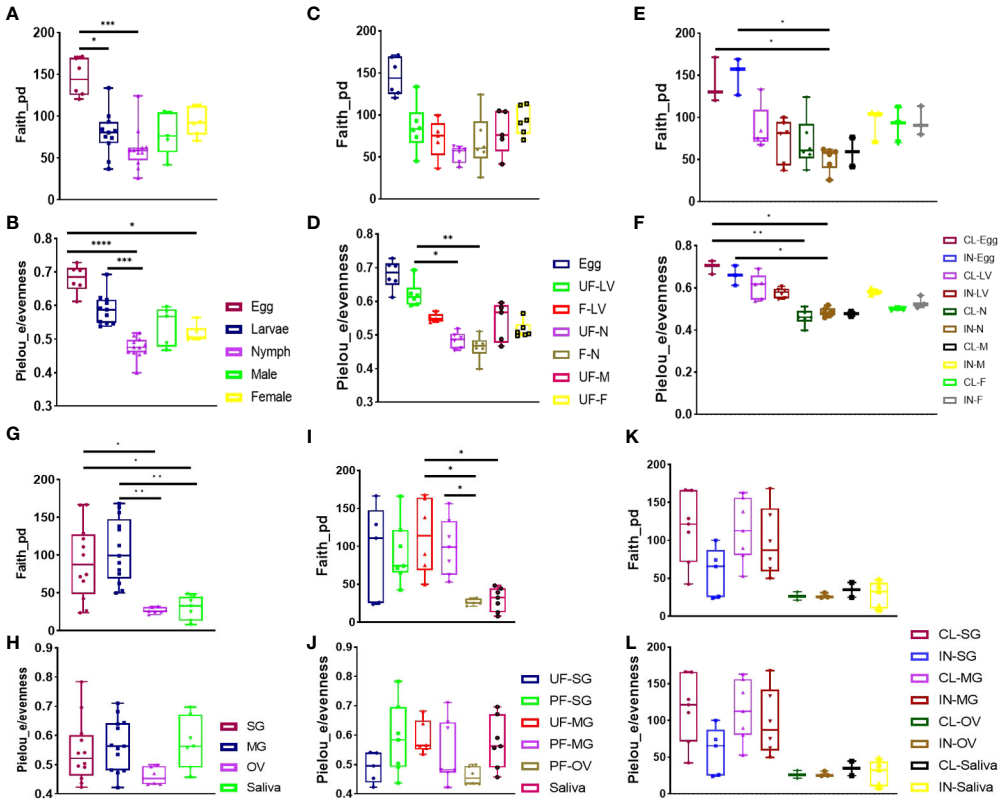

FIGURE 1
Alpha diversity of microbial richness across all developmental stages and isolated tissues. Diversity analysis using Faith phylogenetic distance (species richness) and Pielou_e metrics (evenness) in **(A, B)** all developmental stages, **(C, D)** unfed and fully fed developmental stages, **(E, F)** *R. parkeri*-infected and uninfected developmental stages, **(G, H)** all tissues, **(I, J)** unfed and fully fed tissues, and **(K, L)** *R. parkeri*-infected and uninfected tissues. Each bar on the abundance plot represents average data from 3–5 individual replicates. Each point of the box plots represents average data from 3–5 individual replicates. Unfed (UF), fed (F), larvae (LV), nymph (N), male (M), female (F), clean (CL), infected (IN). Boxplot height indicates the upper and lower quartiles. Whiskers indicate the maximum and minimum values. The black horizontal line indicates the median. Asterisks denote significance (*P < 0.05, **P < 0.01, ***P < 0.001, ****P < 0.0001).

seen to exert a significant impact on species proportions in unfed nymphs when compared with unfed larvae (Kruskal–Wallis test followed by Dunn's multiple comparison test, $p < 0.05$) and in the fed nymphs compared with unfed larvae (Kruskal–Wallis test followed by Dunn's multiple comparison test, $p < 0.001$) when the Pielou_e evenness index was estimated (Figures 1C, D) Overall, blood-feeding had no significant effect on microbial richness compared with unfed ticks across all developmental stages.

The presence of *R. parkeri* infection was not found to affect microbial richness and evenness between the developmental stages. However, a reduction in microbial richness in *R. parkeri*-infected nymphs compared with uninfected eggs and infected eggs was noted (Figure 1E). Significant reduction in specie evenness was observed when uninfected and infected eggs was compared to uninfected and infected nymph respectively (Figure 1F). NMDS analysis of community structure using the Bray–Curtis (BC) distance matrix (PERMANOVA, F-value = 22.818; $R^2 = 0.75015$; p-value < 0.001 [NMDS] Stress = 0.12544) revealed two distinct clustering patterns in which the earlier developmental stage (egg and larvae), were uniquely clustered from the adult tick (male, female) (Additional File, Figure S4). The BC distance matrix measured dissimilarity in microbial communities based on compositional differences among our samples. The observed clustering pattern further supports the differences observed in the presence of *Cutibacterium* in the eggs, larvae, and nymphs but not in adult male and female ticks. Overall, both *Francisella* and *Rickettsia* predominated in the microbiome across all the developmental stages. Both blood meal and *R. parkeri* infection negatively affected the abundance of *Francisella*, while blood meal reduced microbial richness in earlier developmental stages.

Microbiome composition and diversity across tissue niches

As with developmental stages, the phylum Proteobacteria had the greatest abundance of bacteria, with a relative abundance of 86%, followed by Firmicutes, Actinobacteria, and an unknown phylum, as illustrated in the Additional File, Figures S5A–D. Representative sequences generated from salivary gland, midgut and ovarian tissues showed a similar trend to what was found for developmental stages. *Francisella* and *Rickettsia* predominated in the microbiomes of isolated tissues. In addition, the genus *Candidatus_Midichloria* was detected at relatively high abundance across the isolated tissues, except for the saliva microbiome, which contained the genus *Bacillus*. By contrast, the genus *Cutibacterium* was present in all tissues, except for ovarian samples (Additional File, Figure S6A). Following blood uptake, the relative abundances of certain bacteria identified in the partially fed salivary gland was higher than in the unfed salivary gland. Interestingly, blood meal reduced the abundance of *Francisella*, whereas the prevalence of *Rickettsia, Cutibacterium*, and *Candidatus_Midichloria* increased (Additional File, Figure S6B). The effect of blood meal on the microbial abundance in the midgut tissues was different from salivary gland; in the reverse of what was observed in the salivary gland, blood meal increased the relative abundance of *Francisella* and *Candidatus_Midichloria*, while reducing that of *Rickettsia*. Due to the unique developmental trajectory of the female tick, in which ovarian development did not commence until 4–5 days post-blood-feeding, ovarian tissues from unfed female ticks were not included in this analysis (Additional File, Figure S6B). Bacterial communities were significantly different between unfed and partially blood-fed salivary gland (PERMANOVA F-value = 22.766; $R^2 = 0.7779$; p-value < 0.001) and midgut tissues (PERMANOVA F-value = 16.167; $R^2 = 0.69785$; p-value < 0.001), according to PCoA analysis of the Bray–Curtis's distance matrix (Additional File, Figures S7A, B).

The presence of *R. parkeri* was associated with the corresponding increase in the relative abundance of *Candidatus_Midichloria* in all infected compared with uninfected tissues, with the corresponding decrease in the prevalence of *Francisella* (Additional File, Figure S6, Figure 2C). There was an increase in the relative abundance of *Rickettsia* detected in *R. parkeri*-infected saliva compared with saliva from uninfected ticks. Bacterial communities were significantly different between uninfected and infected salivary gland (PERMANOVA F-value = 20.316; $R^2 = 0.75761$; p-value < 0.001), midgut (PERMANOVA) F-value = 36.225; $R^2 = 0.83806$; p-value < 0.001) and ovarian tissues (PERMANOVA F-value = 29.509; $R^2 = 0.89397$; p-value < 0.008), according to PCoA analysis of the Bray–Curtis distance matrix (Additional File, Figures S8A–C).

Overall, microbial richness was highest in midgut tissues (Wilcoxon rank-sum test $p < 0.001$) and lowest in the ovary (Wilcoxon rank-sum test $p < 0.05$), based on the Faith_phylogenetic distance index. At the same time, no significant differences were found in microbial proportions across different tissues, including saliva (Figures 1G, H). The impact of blood meal on alpha diversity between unfed and partially fed tissues was assessed. Unfed midgut tissues had significantly higher specie richness compared to saliva and ovarian tissues, while partially fed midgut tissues displayed a higher species richness compared to the saliva (Figure 1I). We observed no significant effect of blood meal on species proportions (Figure 1J). Similarly, there was no significant difference in either species richness or evenness between *R. parkeri*-infected and uninfected tissues (Figures 1K, L). Here we found that blood meal and *R. parkeri* infection shaped the relative abundance of *Am. maculatum* microbiome in a tissue-dependent manner.

Distinct microbial genera are affected with blood meal or *R. parkeri* infection in developmental stages and tissues

Differential abundance analysis (DAA) was performed on OTU at the genera level to determine which members of the bacterial community were associated with the significant changes blood meal and *R. parkeri* infection. To get the useful information, we selected bacterial genera with overall abundance more than 0.1% to avoid sequencing errors, and any genera for which taxonomy was not available.

Differential abundance analysis (DAA) analysis on the OTU table at genus level indicated higher relative abundance of *Francisella* in female and nymphs, while *Stenotrophomonas* was highest in female and male ticks (Figure 2A). DAA of ticks following *R. parkeri* infection indicated *Francisella* was uniquely abundant in uninfected ticks while *Candidatus_Midichloria* was uniquely abundant in *R. parkeri* infected ticks (Figure 2B). In addition, *Francisella* was least abundant in eggs while *Escherichia, Stenotrophomonas* and *Brachybacterium* were all relatively abundant in unfed female, male and nymph (Figure 2C). DAA of tissue-derived OTUs indicated a higher relative abundance of *Francisella* in ovary and salivary gland while *Rickettsia* was higher in midgut and saliva (Figure 3A). DAA indicated higher relative abundance of *Rickettsia* in unfed and partially fed midgut (Figure 3B). The presence of *R. parkeri* was associated with a higher relative abundance of *Candidatus_Midichloria* and *Rickettsia* in infected tissues and a higher relative abundance of *Francisella* in uninfected tissues following DAA analysis of tissue-derived OTUs (Figure 3C). On the other hand, results of DAA on OTU table at the genus level were in accordance with the observations made about bacterial community structure at the tissue level and indicated the synergism between *R. parkeri* and *Candidatus_Midichloria* and antagonism between *R. parkeri* and *Francisella* (Additional File, Figures S6A-C).

Microbiota interactions across developmental stages

We performed network analysis to visualize significant positive and negative correlations between the bacterial genera identified. We observed a total of 286 significant partial interactions (measure of the degree of relationships between genera) between 43 bacterial genera, 52% (n=150/286) of which showed positive correlations, while the remaining 48% (n=136/286) exhibited negative correlations (Additional File, Table S2). All identified bacteria were from the phyla Actinobacteria (10 genera), Firmicutes (12 genera), Spirochaetota (1 genus), Proteobacteria (12 genera), Cyanobacteria (1 genus), Bacteroidota (4 genera), and Fusobacteria (1 genus) as well as

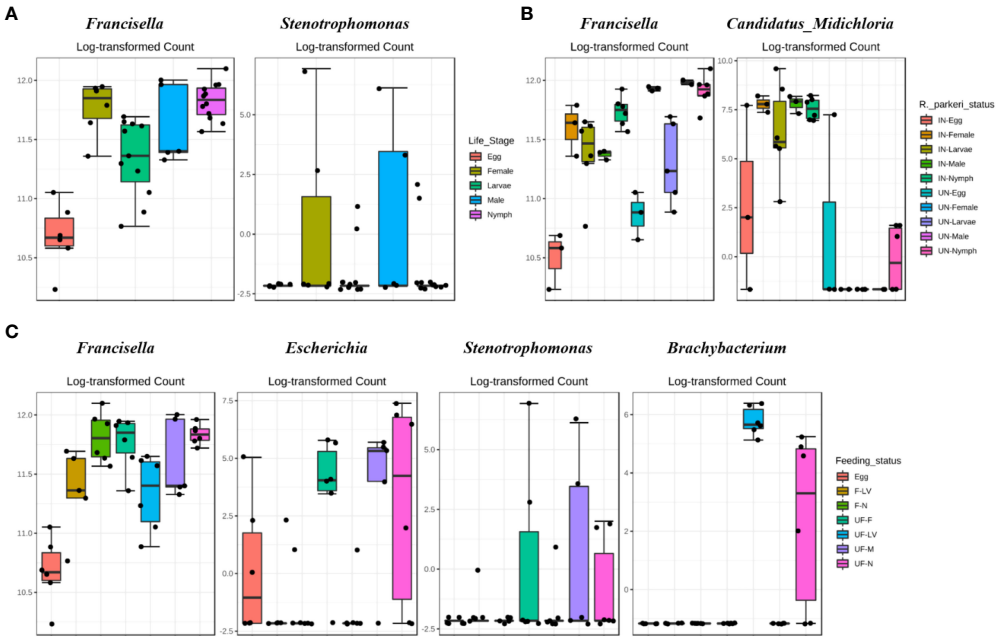

FIGURE 2
DeSeq2 differential abundance analysis of OTUs (genus-level) between **(A)** all life stages **(B)** *R. parkeri* infected and uninfected, and **(C)** unfed and partially fed Am. maculatum. For multiple comparisons an estimate of the FDR was calculated to determine differentially abundant families with a significance threshold of p-value < 0.05. IN (*R. parkeri* infected), UN (uninfected), F (blood fed), UF (unfed).

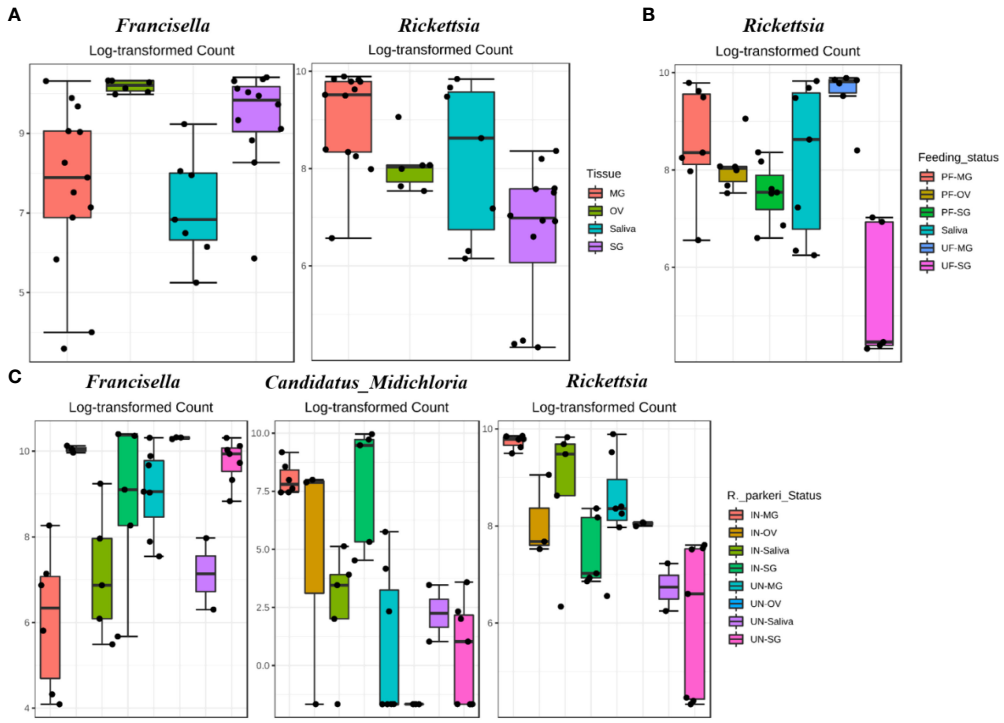

FIGURE 3
DeSeq2 differential abundance analysis of OTUs (genus-level) between **(A)** whole tissues **(B)** *R. parkeri* infected and uninfected, and **(C)** unfed and partially fed Am. maculatum. For multiple comparisons an estimate of the FDR was calculated to determine differentially abundant families with a significance threshold of p-value < 0.05. PF (partially blood fed), UF (unfed), IN (*R. parkeri* infected), UN (uninfected).

an unknown phylum (1 genus) (Figure 4). The genera *Francisella, Rickettsia*, and *Candidatus_Midichloria* were found within the same network cluster where they share significant positive correlations. Individually, they both interacted with other genera as is the case with *Francisella* and *Rickettsia* OTUs sharing negative correlations with *Listeria, Coxiella, Bacillus, and Enterococcus*, and positive correlations with Cutibacterium. The genus *Candidatus_Midichloria* on the other hand was positively correlated with OTUs belonging to the *Mitochondria* genus. It is worth noting that *Candidatus_Midichloria* had fewer taxa with which it interacted than *Francisella or Rickettsia* (Additional File, Table S2). Another interesting observation made from the network interactions was the significant negative correlations in the interactions between *Coxiella* and *Francisella* and between *Coxiella* and *Rickettsia*. A more surprising correlation was identified between *Bacillus, Listeria, Enterococcus*, and *Staphylococcus*, all of which are members of the phylum Firmicutes. They were all negatively correlated with *Rickettsia*, *Francisella*, and *Candidatus_Midichloria* from Proteobacteria (Figure 4).

To identify the significantly represented microbial genera between different life stages, we used linear discriminant analysis effect size (LEfSe) to determine the respective LDA scores for the identified bacteria observed in the samples. LDA analysis showed that, out of 46 bacteria taxa, 13 genera were significantly correlated at different life stages. Several of the bacteria either increased or decreased in more than one life stage. By contrast, the bacterial taxon *Enhydrobacter* is the only genus represented exclusively at the egg stage (Additional File, Table S3). Likewise, the taxa *Enterococcus, Lactobacillus*, and *Coxiella* were not detected at any developmental stages. Another interesting observation was the increased presence of the genera *Corynebacterium* and *Cutibacterium* exclusively at early developmental stages (Additional File, Figure S9).

Tissue-driven microbial interactions

Network analysis in tissues showed 220 significant correlations between 46 bacterial genera, each belonging to the phyla Proteobacteria (20 genera), Firmicutes (13), Actinobacteriota (6 genera), Cyanobacteria (2 genera), Bacteroidota (3 genera), and Fusobacteriota (1 genus) as well as an unknown phylum (1 genus). Seventy-two (33%) were negative correlations, while 148 (67%) were positive correlations (Additional File, Table S4). We observed that OTUs belonging to *Candidatus_Midichloria, Francisella* and *Rickettsia* were

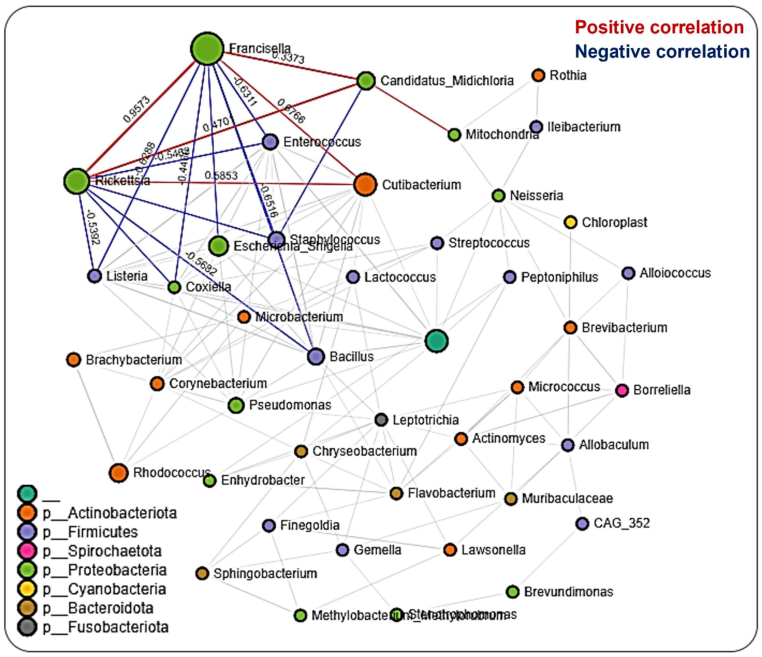

FIGURE 4
Correlation network analysis across the life stages of Am. maculatum ticks. Correlation network generated using the SparCC algorithm. Correlation network with nodes representing taxa at the family level and edges representing correlations between taxa pairs. Node size correlates with the number of interactions in which a taxon is involved, and the line color represents either positive (red) or negative (blue) correlations. The color-coded legend shows the bacterial family to which each taxon belongs.

positively correlated and represent a network cluster that shares both positive and negative correlations with OTUs from other bacteria genera. Interestingly, bacteria belonging to the phylum Firmicutes, such as *Listeria, Staphylococcus, Bacillus, and Enterococcus* were negatively correlated with *Francisella, Rickettsia*, and *Candidatus_Midichloria* which are bacteria from the Proteobacteria phylum (Figure 5). LDA analysis revealed that *Francisella* was significantly enriched in ovaries and salivary glands, whereas *Rickettsia* was increased significantly in the midgut tissues and saliva (Additional File, Table S5; Figure S10). The saliva microbiome was also the only sample exclusively enriched with *Alcaligenes, Moraxella, Pseudomonas*, and *Spiroplasma*. The first three belong to the phylum Proteobacteria and the latter from the phylum Firmicutes.

Microbial interactions in the salivary gland

A total of 608 significant partial interactions between 48 bacteria genera were identified in network analysis of the salivary gland, with 176 (29%) negative correlations and 432 (71%) positive correlations (Additional File, Table S6). Most interactions were seen with *Francisella, Rickettsia*, and *Candidatus_Midichloria* (Figure 6). The most surprising correlation was the negative correlation observed between *Rickettsia* and *Candidatus_Midichloria*, and the most interesting was that *Rickettsia* shares a correlation network only with *Candidatus_Midichloria* (Figure 6). No direct interaction was observed between *Francisella* and *Candidatus_Midichloria* or between *Francisella* and *Rickettsia*. LDA analysis of significantly enriched bacteria revealed a unique pattern between *R. parkeri*-infected and uninfected salivary glands. Uninfected salivary glands were exclusively enriched with *Francisella, Escherichia_Shigella, Cutibacterium*, and Pseudomonas. In contrast, *Candidatus_Midichloria, Enterococcus*, and *Cutibacterium* were the only bacteria significantly enriched in *R. parkeri*-infected salivary glands (Additional File, Figure S11A). Interestingly, *Francisella* was the only bacterium to be significantly enriched in unfed salivary gland. *Francisella* was also enriched in the partially fed salivary gland, albeit at a much lower expression compared to the unfed salivary gland. Several bacteria were also significantly enriched in partially fed salivary gland which include *Escherichia_Shigella, Bacillus, Staphylococcus, Enterococcus, Cutibacterium*, and *Pseudomonas* (Additional File, Figure S11B).

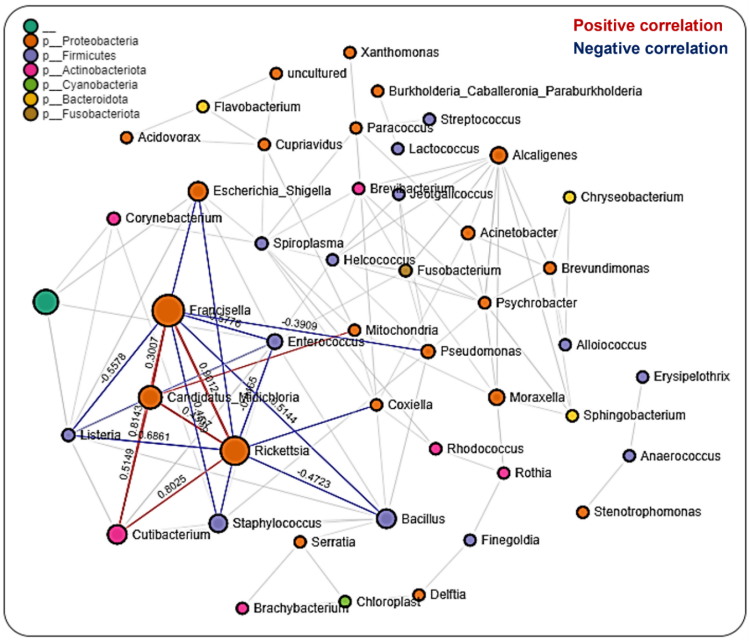

FIGURE 5
Correlation network analysis across tissue stages of *Am. maculatum* ticks. Correlation network generated using the SparCC algorithm. Correlation network with nodes representing taxa at the family level and edges representing correlations between taxa pairs. Node size correlates with the number of interactions in which a taxon is involved, and the line color represents either positive (red) or negative (blue) correlations. The color-coded legend shows the bacterial family to which each taxon belongs.

Microbial interaction in the midgut

We observed many fewer (56) significant partial interactions (measure of the degree of relationships between genera) in the midgut tissues between 29 bacteria genera, all belonging to the phyla Proteobacteria (15 genera), Firmicutes (3 genera), Actinobacteriota (4 genera), Cyanobacteria (1 genus), and Bacteroidota (2 genera) as well as an unknown phylum (1 genus), 16 (29%) of which were negative correlations and the remaining 40 (71%) positive correlations (Additional File, Table S7). The network map of bacterial interactions identified five distinct networks, with *Rickettsia* and *Candidatus_Midichloria* observed to be part of the same network with positive correlations. *Francisella* was found to be in a different network (Figure 7). A striking observation was the ubiquitous presence of bacteria in the phylum Proteobacteria across all five identified networks (Figure 7). The LDA score from LEfSe identified the enrichment of *Rickettsia, Escherichia_Shigella*, and *Cutibacterium* in both uninfected and *R. parkeri*-infected midgut tissues. Compared with the *R. parkeri*-infected midgut, only *Francisella* was significantly enriched in the uninfected midgut, while *Bacillus* was enriched in the *R. parkeri*-infected midgut (Additional File, Figure S11A). Assessing the effect of blood meal on bacterial enrichment identified a shared enrichment of *Rickettsia, Escherichia_Shigella*, and *Cutibacterium* in both unfed and partially fed midgut. We observed *Pseudomonas* and *Brevibacterium* in the unfed midgut, while *Francisella* and *Staphylococcus* were enriched in partially blood-fed midgut tissues (Additional File, Figure S11B). Microbiota–microbiota interactions across developmental stages were driven mainly by three of the most abundant bacteria: *Francisella, Rickettsia*, and *Candidatus_Midichloria*. Other interactions revealed that certain taxonomic groups were inversely correlated, as seen between the phyla Firmicutes and Proteobacteria. Many specific interactions were observed in the tissues, suggesting tissue-dependent influences on how microbes interact in different tissue niches.

Functional characterization of bacterial communities

Functional prediction of microbiota genes compared with COG functional categories identified genes involved in ribosomal structure and biogenesis, nucleotide transport, and metabolism as the most abundant across developmental stages (Additional file, Table S8). Several genes involved in metabolisms, such as lipid transport, coenzyme transport, amino acid transport, and carbohydrate transport, were also identified (Additional files, Figure S12). Prediction of metabolic

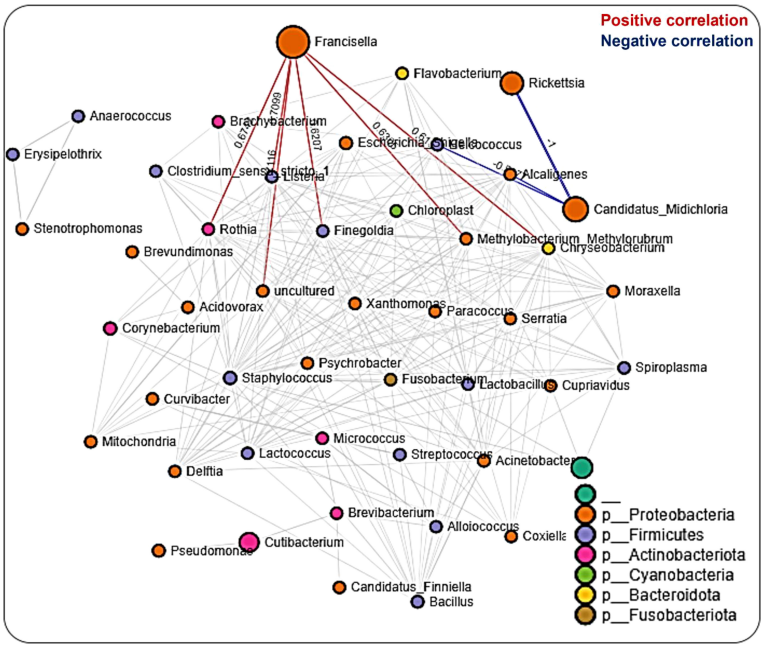

FIGURE 6
Correlation network analysis in the salivary glands of *Am. maculatum* ticks. Correlation network generated using the SparCC algorithm. Correlation network with nodes representing taxa at the family level and edges representing correlations between taxa pairs. Node size correlates with the number of interactions in which a taxon is involved, and the line color represents either positive (red) or negative (blue) correlations. The color-coded legend shows the bacterial family to which each taxon belongs.

genes and pathways using the KEGG Orthology (KO) categories assigned 19% of the metabolic functions to genes in carbohydrate metabolism pathways and 18% of the functions were encoded by genes in amino acid metabolism pathways. By comparison, genes encoding cofactors in the vitamin metabolism pathways and energy metabolism pathways represented 15% and 13% of the metabolic pathways, respectively (Additional file, Figure S12).

Differences in functional community profiles within the metabolic pathways were further examined between the different feeding stages and infection status across dissected tissues based on the KEEG metabolism categories. The partially fed salivary gland and midgut had a higher proportion of sequences assigned to energy metabolism and carbohydrate metabolism than the unfed salivary gland and midgut (Figures 8A, B). The presence of *R. parkeri* led to an increase in the proportion of glycan biosynthesis and metabolism genes, carbohydrate metabolism genes, and genes involved in the metabolism of cofactors and vitamins in the salivary glands. A slight increase was also seen in genes involved in the metabolism and biodegradation of xenobiotic in the *R. parkeri*-infected salivary gland (Figure 9A). A slight increase in the proportion of energy metabolism genes was associated with *R. parkeri* in infected midgut compared with the uninfected midgut (Figure 9B). Interestingly, genes involved in amino acid metabolism were seen to be reduced in *R. parkeri*-infected salivary glands and midgut compared with uninfected tissues (Figures 9A, B). No differences between metabolic predictions were detected between *R. parkeri*-infected and uninfected ovarian tissues (Additional file, Figure S13).

Discussion

This study is the first to characterize microbiome changes throughout the ontogeny of the Gulf Coast tick, a competent vector of the spotted fever group rickettsiae, *R. parkeri*. Using a high-throughput metagenomic approach that allowed us to barcode DNA extracted from individual ticks and process them in a single run, the present study set out with the aim of assessing the core microbial assemblages present in *Am. maculatum* ticks and determine the changes under certain physiological conditions vis-à-vis development, hematophagy, and pathogen infection. The results show that changes to the core microbiome occur in response to a blood meal and pathogen association but not as a function of the developmental stage. Similarly, as expected, microbe-microbe interactions depended on the specific tick tissues in which those interactions took place.

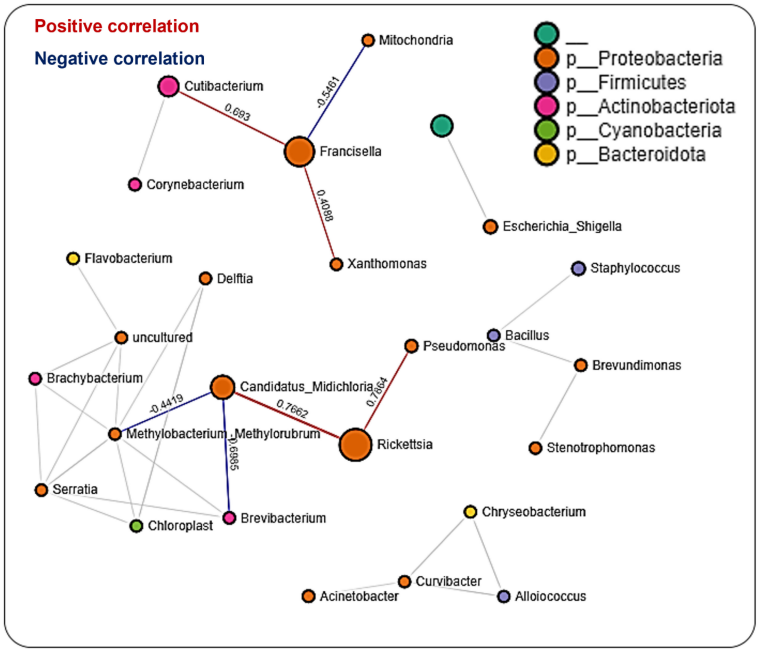

FIGURE 7
Correlation network analysis in the midgut of *Am. maculatum* ticks. Correlation network generated using the SparCC algorithm. Correlation network with nodes representing taxa at the family level and edges representing correlations between taxa pairs. Node size correlates with the number of interactions in which a taxon is involved, and the line color represents either positive (red) or negative (blue) correlations. The color-coded legend shows the bacterial family to which each taxon belongs.

The *Amblyomma maculatum* microbiome remains stable across ontogeny

The typical life cycle of *Am. maculatum* ticks encompass critical physiological and environmental events conferred by intrinsic and extrinsic factors, such that the persistence of the microbiome and every similar micro-community that utilizes the tick as a microenvironment across these dynamic events is continuously tested. Two very well-studied factors that exert significant pressure on the tick microbiome are blood meal and pathogen replication (Abraham et al., 2017; Swei and Kwan, 2017; Adegoke et al., 2020; Wei et al., 2021), albeit with varying outcomes reported. In the current study, a shift favoring the establishment of a single bacterial genus along developmental lines (eggs to adult male and female) is exhibited (Additional File, Figures S3A–C). Even so, the uptake and breakdown of nutritious blood meals and the intricacies of tick–pathogen interactions involve several detailed mechanistic processes that have been shown to significantly impact tick physiology (de la Fuente et al., 2016; Hoxmeier et al., 2017; Budachetri et al., 2018), the current study shows that members of the *Am. maculatum* microbial communities exhibit reduced plasticity thus maintaining a stable microbial core. This observation raises the question of whether the tick microbiome is self-regulated in ticks and tick tissues.

Notably, while the core microbiome persists across developmental stages, certain bacterial genera were found to be associated with both blood meal and pathogen infection, as seen with *Cutibacterium* and *Candidatus_Midichloria*, and whether the introduction of these bacteria in fewer numbers significantly impacts overall tick biology is a question beyond the scope of this study (Abraham et al., 2017; Budachetri et al., 2018; Adegoke et al., 2020). To further understand how changes across tick developmental stages shape microbial assemblages, it is imperative to assess microbial assemblages and community measures of diversity, such as richness and evenness (Brown et al., 2020). Community diversity is important because the smallest differences at the taxon level induced by blood meal or pathogen interaction could interfere with community structure, which would otherwise not be reflected in the abundance profile. We observed a continuous decrease in community diversity towards later developmental stages (Figures 2A-F). For both diversity metrics employed, a reduction in community richness likely indicated the corresponding decline in all or certain specific bacterial taxa. At the same time, a decrease in evenness would imply that certain bacterial taxa are allowed to increase in abundance at the expense of other bacteria. This finding is

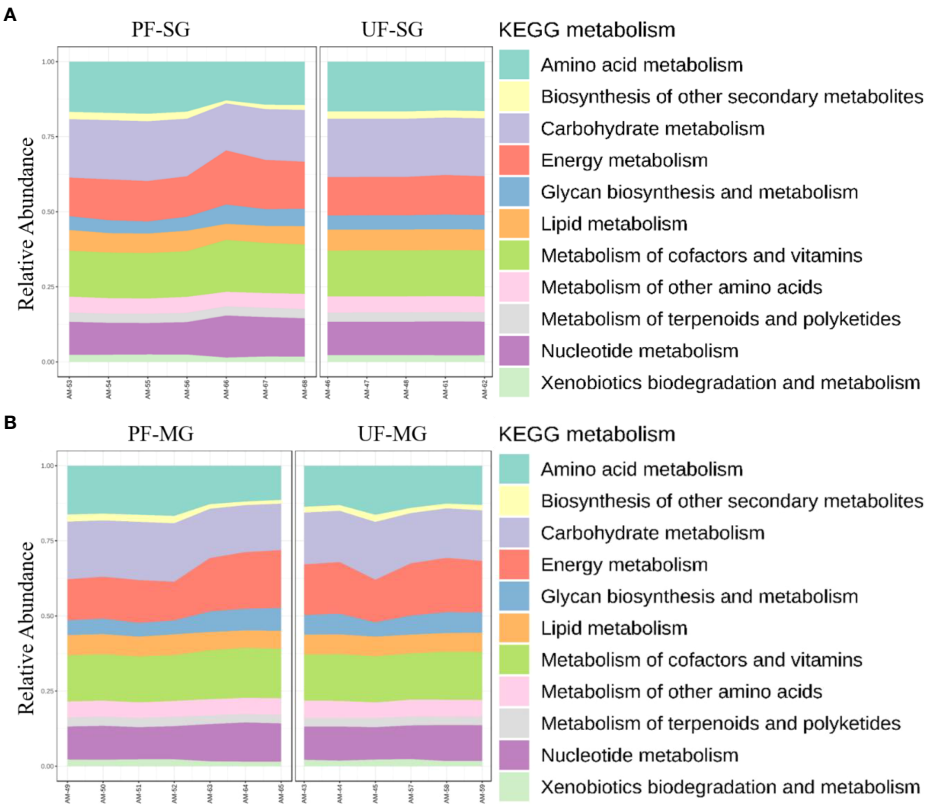

FIGURE 8
Histogram indicating the functional differences between the fed and partially fed Am. maculatum microbiota in **(A)** salivary gland and **(B)** midgut tissues. KEGG metabolic categories were obtained from 16S rRNA gene sequences using the PICRUSt2 pipeline.

consistent with observations made in the kissing bugs, where there is a decrease in diversity associated with ontogenic development (Mann et al., 2020), which is in disagreement with Oliveira et al. (2018), who reported an increase in diversity with ontogenic development. A possible explanation for this discrepancy may be attributed to internal and external changes that occur during metamorphosis. Shedding of the midgut lining and the external cuticles are two of the most important phenomena during development. These may come with significant loss of resident and non-obligate bacteria whose absence poses no detrimental effect on tick biology (Engel and Moran, 2013). There are, however, other possible explanations for the reduction in diversity seen in this study. One such explanation is that bacteria that are not vertically maintained from the female to her eggs are replaced by vertically maintained bacteria. The preservation of vertically maintained species would explain the loss of *Cutibacterium* in adult male and female ticks. By extension, there would be a reduction in overall diversity. Previous findings have highlighted the importance of initial exposure to bacteria in eliciting a robust immune response upon subsequent exposure to the same bacteria or bacteria from a similar group, a phenomenon referred to as immune priming (Trappeniers et al., 2019; Powers et al., 2020). This could explain the fact that immature developmental stages of ticks are easily infected with bacteria from the environment because of their naïve immune status. These bacteria will not be carried over to the adult stage due to a more developed immune status. The persistence of *Francisella, Rickettsia*, and *Candidatus_Midichloria* to the adult male and female further emphasizes their position as candidates for vertical maintenance, as previously reported for bacterial species from the same genus (Baldridge et al., 2009; Wright et al., 2015; Azagi et al., 2017; Mukhacheva and Kovalev, 2017; Budachetri et al., 2018).

Microbial assemblages in tissues are driven by pathogen and host blood

To gain in-depth insight into how different arthropod tissues contribute to tick biology and, most importantly, their role in vector competence, it is imperative to know how resident microbial communities differ from one tissue to the other. Several factors have been identified that significantly affect how the microbiome is shaped in different arthropod tissues, albeit with varying outcomes and findings. In this study, we

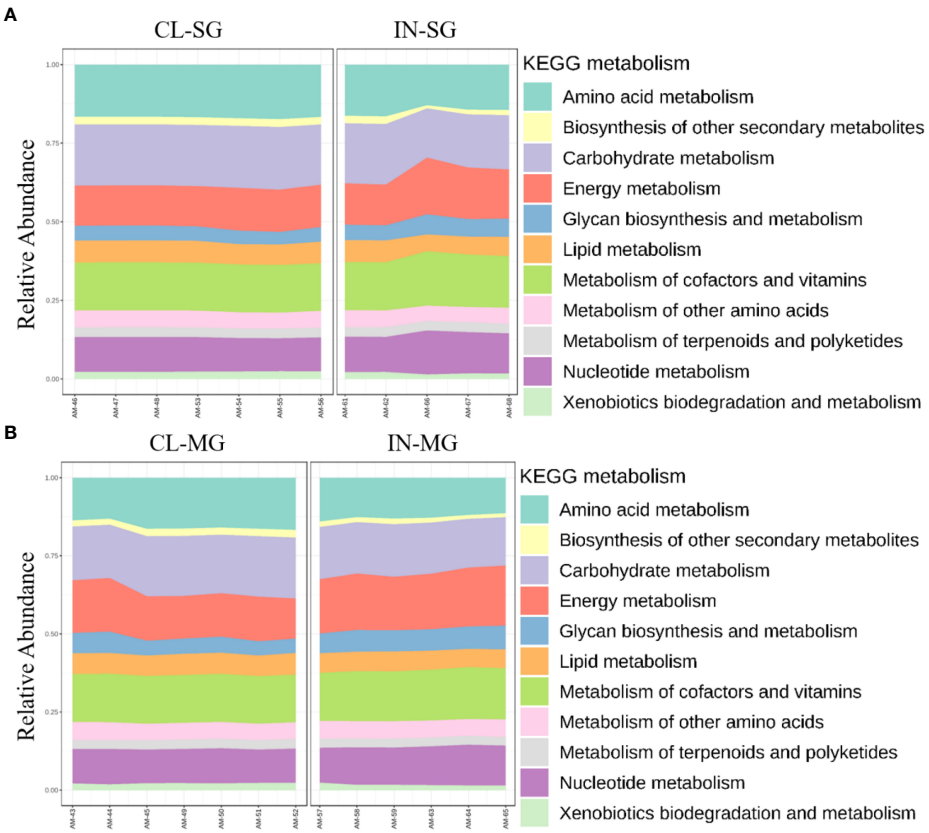

FIGURE 9
Histogram indicating the functional differences between the uninfected and R. parkeri-infected Am. maculatum microbiota in **(A)** salivary gland and **(B)** midgut tissues. KEGG metabolic categories were obtained from 16S rRNA gene sequences using the PICRUSt2 pipeline.

asked whether differences in microbial composition occur within tissues and whether changes influence these differences in the state of blood-feeding and infection status. Our results clearly show a difference in the abundance and composition of the bacteria identified across tick tissues. A conclusion from our findings is the higher bacterial proportion in saliva, which does not correspond to the bacterial balance in the salivary glands. Tick saliva simply contains a snapshot of the microbes secreted by the tick and is possibly not a good representation of all microbes delivered during prolonged feeding. These differences can be explained in part by the fact that some of the microbial populations identified in the saliva, such as *Bacillus* and *Staphylococcus*, are known environmental bacteria, have also been reported to be found on the skin and fur of the animal hosts (Dastgheyb and Otto, 2015; Onyango and Alreshidi, 2018; Ravine, 2019), and may have been acquired during the feeding process. Some of these bacteria could also have been mechanically transferred during saliva collection from the ticks. The presence of the microbiome within tick saliva, while preliminary, could implicate the tick microbiome in modulating the host immune response to tick bite at the host–tick interface.

The observation of a higher diversity seen in midgut tissues compared with salivary gland, ovary, and saliva contrasted with the findings of Zolnik et al. (2016), who reported a higher diversity in salivary gland compared with midgut tissue. The tick midgut and associated peritrophic membrane play an important role in blood breakdown and its components by several catalytic proteins. The production of toxic reactive oxygen species (ROS) and reactive nitrogen species (RNS), which follow blood digestion, is also dampened by these midgut proteins, thus enabling midgut-resident microbial replication. The heme component of the blood meal derived by catalytic proteins also counters the potential tissue damage associated with a heme-induced oxidative burst. Another plausible explanation for the higher microbial diversity observed in the midgut reported from this study is that the midgut is the only tissue that directly encounters host blood, and it provides the first line of contact with any bacterium coming in with the blood meal (Houk, 1977; Tarnowski and Coons, 1989; Gaio et al., 2011; Lejal et al., 2019). However, prolonged blood feeding and, by extension, the initiation of blood meal digestion might provide an enabling environment for bacterial replication

and growth, hence impacting the dynamic and increasing overall diversity of the midgut microbiome as seen from this study. Due to the importance of the ovarian tissues in developmental success, it is expected that several physiological barriers will be put in place to confer protection and reduce the tick's interaction with circulating microbes to the barest minimum. The reduced microbial diversity observed in the ovary is consistent with this, as seen in Figure 1G. Several studies have outlined the contribution of invertebrate hemocytes to immune functions while also identifying distinct populations of hemocytes as either circulating or sessile (Kadota et al., 2003; King and Hillyer, 2013; Sigle and Hillyer, 2018). The sessile population of hemocytes is usually found attached to cavity walls, such as the abdomen, thorax, and internal organs. While extensive studies have described how arthropod hemocytes play a significant role in immunomodulation (Pereira et al., 2001; Hillyer, 2009; Liu et al., 2011; Hillyer and Strand, 2014; Fiorotti et al., 2019; Kwon and Smith, 2019), few studies have defined the functional role of sessile populations in the biology of the organism (Sigle and Hillyer, 2016). Hence, it could be hypothesized that circulating or sessile hemocytes would form immunological barriers as part of an extensive physiological barrier to protect a vital organ, such as the ovary, as seen with several human and mammalian blood–tissue barriers (Fröhlich, 2002)

It has already been established that blood uptake, which usually lasts several days in ticks, can introduce a plethora of pathogenic and non-pathogenic microbes into ticks (Bhatia et al., 2018; Zolnik et al., 2018; Landesman et al., 2019). While ticks acquire host blood for nutritional requirements, several host factors present in the blood meal could also potentially contribute to compositional changes that are likely to occur to the microbiome throughout the extended feeding process. For instance, the tick midgut responds to the presence of the blood meal *via* intricate protein expression patterns (Rachinsky et al., 2008; Schwarz et al., 2014; Perner et al., 2016; Oleaga et al., 2017; Liu et al., 2018) while also undergoing certain morphological and structural adjustments (Tarnowski and Coons, 1989; Franta et al., 2010), all of which could have an impact on the microbial environment in the midgut, as previously reported (Zhang et al., 2014; Zolnik et al., 2018; Landesman et al., 2019). Results from our study show that microbial diversity is impacted following uptake of the blood meal in both salivary gland and midgut tissues (Figure 1K). We also observed a combinatorial effect of blood meal and *R. parkeri* infection in reducing the abundance of *Francisella* while increasing *Rickettsia* abundance in the partially fed and infected salivary gland and, vice-versa, in the partially fed and infected midgut. This suggests that there is the trafficking of *Rickettsia* from the midgut into the salivary gland during feeding. While studies that assessed the impact of blood meal on the tick microbiome are limited to developmental stages, it is interesting to note that our studies corroborate a great number of these studies, albeit in life stages. Zolnik and colleagues (2016) observed a significant reduction in alpha-diversity throughout the feeding period of nymphal ticks compared with the unfed nymphs of black-legged ticks, and Zhang et al. (2014) also reported an altered microbial composition following a prolonged blood meal in *Ixodes persulcatus* ticks. A similar observation was reported in the malaria mosquito, in which Muturi et al. (2019) found a significant decrease in microbial diversity in blood-fed *Aedes aegypti* compared with sugar-fed *Ae. aegypti* mosquitoes. While comparing the effect of different host blood meal sources was beyond the scope of this study, our findings strongly implicate host blood meal as a significant factor in driving tick microbiome diversity, which may pose a significant effect on tick biology, as previously shown by Swei and Kwan, 2017.

Microbe–microbe interactions are driven by the specific host tissue and not the developmental stage

Microbial interactions across developmental stages

The biological success of the tick as a hematophagous arthropod and a vector of disease pathogens hinges partly on the specific interactions between different members of the resident microbiota, which encompasses the entirety of all the microorganisms present in an environment. Identifying unique interactions between these microbial community members is a critical step in developing effective control measures against tick-transmitted pathogens.

Our network analysis on the overall dataset across all developmental stages identified similar percentages of positive and negative correlations, suggesting a much more balanced distribution of both antagonistic (Budachetri et al., 2018) and synergistic (Eiler et al., 2012; Chow et al., 2014) interactions between members of the microbial communities. This observation contrasts with a recent study by Lejal et al. (2021), who reported more than 97% partial positive correlations across all the datasets in *Ixodes ricinus* ticks and suggested that most of the tick microbial community favors a mutualistic interaction. While the findings of our study contrast with this observation, it should be stated that microbial correlations of an individual organism may not fully represent interactions in different tissue niches, which are often a microenvironment for unique bacteria communities (Pollet et al., 2020). The genera *Rickettsia*, *Francisella*, and *Candidatus_Midichloria* were all part of the same network, with positive correlations between all three bacterial genera, and these were previously identified in *Am. maculatum* ticks (Budachetri et al., 2014; Budachetri et al., 2018) and *Ix. ricinus* ticks (Lejal et al., 2021). At the same time, *Francisella* and *Candidatus_Midichloria* are major endosymbionts found across all developmental stages and tissues (salivary gland, midgut and ovaries) of *Am. maculatum* microbiome and Budachetri et al. (2018) reported an increase in

Candidatus_Midichloria load following *R. parkeri* infection, proposing a positive correlation between these bacteria and the corresponding reduction in *Francisella* load following *R. parkeri* infection, implying a negative correlation.

Interestingly, recent network analysis on the *Ix. ricinus* microbiota also shows a positive correlation between *Rickettsia* and *Candidatus_Midichloria* OTUs, indicating a facilitative interaction between these bacteria (Lejal et al., 2021). Our data suggest a positive interaction between the pathogenic Rickettsia and the obligate endosymbiont *Candidatus_Midichloria*. The current study's findings are consistent with those of Budachetri et al. (2018), who reported a synergistic interaction between *R. parkeri* and *Candidatus_Midichloria mitochondrii* and an antagonistic interaction between *R. parkeri* and a *Francisella*-like endosymbiont. While identification at the species level exceeded the resolution of our sequencing analysis, we have strong reason to believe that the OTU belonging to the *Coxiella* genus is the *Coxiella*-like endosymbiont (CLE), because the ticks used in this study were strictly maintained under laboratory conditions. CLE is ubiquitously present in most hard ticks, with reports suggesting an obligate association with the tick host, in which they provide essential vitamin supplements for tick physiological success (Duron et al., 2015; Smith et al., 2015; Guizzo et al., 2017; Ben-Yosef et al., 2020).

A recent study reported the replacement of bacteria in the *Coxiellaceae* family with those in the *Francisellaceae* family in both lab-maintained and field-*collected Am. americanum* ticks (Kumar et al., 2022), providing further evidence of competition between these two tick endosymbionts. The strict adherence to a single nutritional mutualist by tick species is an area of tick–microbial interaction that requires further exploration, and future studies should aim at characterizing both the immunoproteome and metabolites of gnotobiotic ticks with known obligate endosymbionts. Other key interactions observed between the OTUs belong to the *Bacillus*, *Rickettsia*, and *Francisella* genera. The genus *Bacillus* is an environmental resident microbe that ticks acquire while questing in the environment and during the attachment process to the host (Ross et al., 2019). We observed negative correlations between *Bacillus* and *Rickettsia* and between *Bacillus* and *Francisella*, suggesting a competitive interaction between these bacterial OTUs. The findings of the current study are consistent with those of another study (Lejal et al., 2021) that described a positive correlation between *Bacillus* and *Rickettsia* but was not compatible with the presence of a high abundance of *Bacillus* in *Theileria*-positive *Rhipicephalus microplus* ticks, as previously described (Adegoke et al., 2020). The factors that favor the establishment and long-term association of environmentally acquired bacteria by ticks still need to be experimentally identified. Whether these bacteria express effector molecules that suppress pathogenic microbes, such bacteria may be utilized as effective vector-control tools in the future to develop paratransgenic ticks.

Microbial interactions are driven by the specific tissue niche

Network analysis on datasets representing all tissues was initially carried out, thereby identifying 67% positive correlations between different bacteria in the networks. We identified more positive correlations across tissue levels than developmental stages, suggesting a much finer association scale at smaller niches (Pollet et al., 2020). Aside from the higher proportion of positive correlations, most of the microbial networks identified when applied to the combined tissue dataset were like those presented for developmental stages. For instance, OTUs from *Francisella, Rickettsia, and Candidatus_Midichloria* were all present in the combined tissue networks, including the salivary gland and midgut. Interestingly, while the salivary gland dataset had a relatively higher proportion of networks, it contained more positive correlations (71%). Only OTUs belonging to the genera *Francisella, Rickettsia*, and *Candidatus_Midichloria* were involved in most interactions. An unexpected outcome from the salivary gland network was the observation of a negative correlation between *Rickettsia* and *Candidatus_Midichloria* OTUs, while there was no direct correlation between *Francisella* and either of *Rickettsia* or *Candidatus_Midichloria*. We proposed that *Candidatus_Midichloria* in the salivary gland was not transmitted to the host, due to its restricted location in the mitochondria, hence its absence from the saliva. This phenomenon was also observed in the midgut, albeit with fewer and more distinctly separated microbial networks. A handful of studies deciphered specific correlations between microbial members residing in arthropod vectors (Lejal et al., 2021; Hegde et al., 2018). While our findings here are preliminary at best, they emphasize that tissue-specific microbial interactions do exist, and this should be further investigated, as they may lead to new insights into pathogen replication and establishment across tick tissues. Future work should be targeted towards experimental validation of the predicted correlations to understand how these interactions are shaped.

The metabolic predictions based on the microbiota showed no differences in metabolic genes across developmental stages; however, we identified a diverse category of genes involved in metabolic pathways, most of which have been previously reported in ticks and other blood-feeding arthropods (Bahrndorff et al., 2018; Obregón et al., 2019; Couper et al., 2019; Jing et al., 2020). The presence of energy metabolism genes and pathways in higher abundance in the partially fed than the unfed salivary gland and midgut tissues did not completely align with the microbial changes induced by blood meal, especially with the midgut. We saw a significant increase in the microbial profiles in the partially fed salivary gland compared with the unfed salivary gland (Additional File, Figure S6B). We hypothesize that since the increased proportion of bacterial genes was involved in energy metabolism, carbohydrate

metabolism could be a physiological pressure on the salivary gland as a secretory organ involved in blood meal at the host–feeding interface. The slight increase in the number of genes involved in xenobiotic degradation and metabolism in the partially fed salivary gland could be due to the constant need to counter host immune responses to achieve hematophagy.

Interestingly, metabolic pathways involved in energy metabolism and the metabolism of vitamins and cofactors were upregulated in *R. parkeri*-infected salivary glands and midgut tissues (Figures 9A, B). These changes were also similar to those associated with uptake of blood meal. While we could not tease out whether these changes were solely associated with either blood meal or *R. parkeri* infection, we saw a slight increase in the abundance of genes involved in nucleotide metabolism pathways in the *R. parkeri*-infected salivary gland. The importance of nucleotide metabolism pathways in bacteria is highlighted by their role in bacterial physiological processes and the synthesis of new nucleic acids necessary for replication (DNA) and transcription (RNA) (Lopatkin and Yang, 2021). Our current results show that blood meal increases the relative abundances of *Francisella* and *Candidatus_Midichloria* endosymbionts. Likewise, the abundance of *Rickettsia* also increases with *R. parkeri* infection, suggesting an overall increase in the replication of these bacterial groups, thus leading to an overall increase in nucleic acid replication and transcription. While our functional analysis is predictive at best, with approximately 85% similarity with shotgun metagenomics, it did provide comprehensive insight into the different functional pathways present in the tick microbiota.

Conclusions

The core microbiome of *Am. maculatum* comprises ten bacterial genera. Three genera, including *Rickettsia, Francisella*, and *Candidatus_Midichloria*, predominate in the core microbiome. Blood-feeding behavior aided to increase the relative abundances of these three bacteria, whereas overall diversity and evenness were reduced due to elevated levels of ROS associated with blood meal acquisition and digestion, both in whole ticks and in particular organs (gut/salivary glands/ovaries). *R. parkeri* infection co-proliferates with *Candidatus_Midichloria*, while an antagonistic interaction with the *Francisella* genus was observed in the tick life cycle. *R. parkeri* infection further increased the diversity or evenness of the core microbiome. A significant increase in the presence of genes related to metabolic pathways was observed in ticks after a blood meal and pathogen infection. With these results in mind, further study should focus on the interplay between these three bacterial species, including the pathogen, while studying tick–pathogen interactions. The interplay of symbiotic bacteria (*Candidatus_Midichloria/Francisella*) with pathogenic *R. parkeri* should yield important findings in future studies.

Data availability statement

The datasets presented in this study can be found in online repositories. The names of the repository/repositories and accession number(s) can be found below: https://www.ncbi.nlm.nih.gov/genbank/, PRJNA774067; https://datadryad.org/stash, https://doi.org/10.5061/dryad.r2280gbgg.

Ethics statement

The animal study was reviewed and approved by The University of Southern Mississippi IACUC.

Author contributions

Conceptualization: SK. Data curation: AA, DK, and SK. Formal analysis: AA, DK, and SK. Funding acquisition: SK. Investigation: AA and SK. Methodology: AA, DK, and KB. Project administration: SK. Resources: SK. Supervision: SK.Validation: AA and SK. Visualization: AA. Writing, original draft: AA and SK. Writing, review & editing: AA, DK, KB, and SK. All authors contributed to the article and approved the submitted version.

Funding

This research was principally supported by USDA NIFA Award # 2017-67017-26171, Pakistan-US Science and Technology Cooperation award (US Department of State), NIH NIAID award # R15AI099910, NIH NIGMS Award # R15GM123431, and the Mississippi INBRE (an institutional Award (IDeA) from the National Institute of General Medical Sciences of the National Institutes of Health under award P20GM103476). The funders played no role in the study design, data collection, analysis, publication decision, or manuscript preparation.

Acknowledgments

The authors thank Surendra Raj Sharma, Latoyia Downs, and Faizan Tahir for thought-provoking and enriching discussions, particularly about endosymbionts, reproductive

fitness, and priming of the tick immune system. Finally, we are grateful to Dr. Michael Garrett, UMMC genomics core facility.

Conflict of interest

The authors declare that the research was conducted in the absence of any commercial or financial relationships that could be construed as a potential conflict of interest.

Publisher's note

All claims expressed in this article are solely those of the authors and do not necessarily represent those of their affiliated organizations, or those of the publisher, the editors and the reviewers. Any product that may be evaluated in this article, or claim that may be made by its manufacturer, is not guaranteed or endorsed by the publisher.

Supplementary material

The Supplementary Material for this article can be found online at: https://www.frontiersin.org/articles/10.3389/fcimb.2022.1037387/full#supplementary-material

SUPPLEMENTARY FIGURE 3
Stability of bacterial abundances across developmental stages. The relative abundances of the predominant members of microbial communities in **(A)** all developmental stages, **(B)** unfed and fully fed developmental stages and **(C)** *R. parkeri*-infected and uninfected developmental stages. Each bar on the abundance plot represents average data from 3–5 individual replicates. Unfed (UF), fed (F), larvae (LV), nymph (N), male (M), female (F), clean (CL), infected (IN).

SUPPLEMENTARY FIGURE 6
Changes in microbial assemblages and diversity across different tissues. The relative abundances of the predominant members of microbial communities in **(A)** all isolated tissues, **(B)** unfed and fully fed tissues, and **(C)** *R. parkeri*-infected and uninfected tissues. Each bar on the abundance plot represents average data from 3–5 individual replicates. Unfed (UF), fed (F), larvae (LV), nymph (N), male (M), female (F), clean (CL), infected (IN), salivary gland (SG), midgut (MG), ovary (OV).

References

Abraham, N. M., Liu, L., Jutras, B. L., Yadav, A. K., Narasimhan, S., Gopalakrishnan, V., et al. (2017). Pathogen-mediated manipulation of arthropod microbiota to promote infection. *Proc. Natl. Acad. Sci. U. S. A.* 114 (5), E781–E790. doi: 10.1073/pnas.1613422114

Adams, J. F. (1963). Biological half-life of vitamin B12 in plasma. *Nature* 198, 200. doi: 10.1038/198200a0

Adegoke, A., Kumar, D., Bobo, C., Rashid, M. I., Durrani, A. Z., Sajid, M. S., et al. (2020). Tick-borne pathogens shape the native microbiome within tick vectors. *Microorganisms* 8 (9), 1299. doi: 10.3390/microorganisms8091299

Azagi, T., Klement, E., Perlman, G., Lustig, Y., Mumcuoglu, K. Y., Apanaskevich, D. A., et al. (2017). Francisella-like endosymbionts and rickettsia species in local and imported hyalomma ticks. *Appl. Environ. Microbiol.* 83 (18), e01302–e01317. doi: 10.1128/AEM.01302-17

Bahrndorff, S., de Jonge, N., Hansen, J. K., Lauritzen, J., Spanggaard, L. H., Sørensen, M. H., et al. (2018). Diversity and metabolic potential of the microbiota associated with a soil arthropod. *Sci. Rep.* 8, 2491. doi: 10.1038/s41598-018-20967-0

Baldridge, G. D., Scoles, G. A., Burkhardt, N. Y., Schloeder, B., Kurtti, T. J., and Munderloh, U. G. (2009). Transovarial transmission of francisella-like endosymbionts and anaplasma phagocytophilum variants in dermacentor albipictus (Acari: Ixodidae). *J. Med. Entomol.* 46 (3), 625–632. doi: 10.1603/033.046.0330

Ben-Yosef, M., Rot, A., Mahagna, M., Kapri, E., Behar, A., and Gottlieb, Y. (2020). Coxiella-like endosymbiont of rhipicephalus sanguineus is required for physiological processes during ontogeny. *Front. Microbiol.* 11. doi: 10.3389/fmicb.2020.00493

Bhatia, B., Hillman, C., Carracoi, V., Cheff, B. N., Tilly, K., and Rosa, P. A. (2018). Infection history of the blood-meal host dictates pathogenic potential of the Lyme disease spirochete within the feeding tick vector. *PloS Pathog.* 14 (4), e1006959. doi: 10.1371/journal.ppat.1006959

Bolyen, E., Rideout, J. R., Dillon, M. R., Bokulich, N. A., Abnet, C. C., Al-Ghalith, G. A., et al. (2019). Reproducible, interactive, scalable and extensible microbiome data science using QIIME 2. *Nat. Biotechnol.* 37, 852–857. doi: 10.1038/s41587-019-0209-9

Bonnet, S. I., Binetruy, F., Hernández-Jarguín, A. M., and Duron, O. (2017). The tick microbiome: Why non-pathogenic microorganisms matter in tick biology and pathogen transmission. *Front. Cell. Infect. Microbiol.* 7. doi: 10.3389/fcimb.2017.00236

Bonnet, S. I., and Pollet, T. (2021). Update on the intricate tango between tick microbiomes and tick-borne pathogens. *Parasit. Immunol.* 43 (5), e12813. doi: 10.1111/pim.12813

Boulanger, N., and Wikel, S. (2021). Induced transient immune tolerance in ticks and vertebrate host: A keystone of tick-borne diseases? *Front. Immunol.* 12. doi: 10.3389/fimmu.2021.625993

Brinkerhoff, R. J., Clark, C., Ocasio, K., Gauthier, D. T., and Hynes, W. L. (2020). Factors affecting the microbiome of ixodes scapularis and amblyomma americanum. *PloS One* 15 (5), e0232398. doi: 10.1371/journal.pone.0232398

Brown, J. J., Rodríguez-Ruano, S. M., Poosakkannu, A., et al. (2020). Ontogeny, species identity, and environment dominate microbiome dynamics in wild populations of kissing bugs (Triatominae). *Microbiome* 8, 146. doi: 10.1186/s40168-020-00921-x

Budachetri, K., Browning, R. E., Adamson, S. W., Dowd, S. E., Chao, C. C., Ching, W. M., et al. (2014). An insight into the microbiome of the amblyomma maculatum (Acari: Ixodidae). *J. Med. Entomol.* 51 (1), 119–129. doi: 10.1603/me12223

Budachetri, K., and Karim, S. (2015). An insight into the functional role of thioredoxin reductase, a selenoprotein, in maintaining normal native microbiota in the gulf coast tick (Amblyomma maculatum). *Insect Mol. Biol.* 24 (5), 570–581. doi: 10.1111/imb.12184

Budachetri, K., Kumar, D., Crispell, G., Beck, C., Dasch, G., Karim, S., et al. (2018). The tick endosymbiont candidatus midichloria mitochondrii and selenoproteins are essential for the growth of rickettsia parkeri in the gulf coast tick vector. *Microbiome* 6, 141. doi: 10.1186/s40168-018-0524-2

Budachetri, K., Kumar, D., and Karim, S. (2017). Catalase is a determinant of the colonization and transovarial transmission of rickettsia parkeri in the gulf coast tick amblyomma maculatum. *Insect Mol. Biol.* 26 (4), 414–419. doi: 10.1111/imb.12304

Callahan, B. J., McMurdie, P. J., Rosen, M. J., Han, A. W., Johnson, A. J., and Holmes, S. P. (2016). DADA2: High-resolution sample inference from illumina amplicon data. *Nat. Methods* 13 (7), 581–583. doi: 10.1038/nmeth.3869

Chong, J., Liu, P., Zhou, G., and Xia, J. (2020). Using microbiome analyst for comprehensive statistical, functional, and meta-analysis of microbiome data. *Nat. Protoc.* 15, 799–821. doi: 10.1038/s41596-019-0264-1

Chow, C.-E. T., Kim, D. Y., Sachdeva, R., Caron, D. A., and Fuhrman, J. A. (2014). Top-down controls on bacterial community structure: Microbial network analysis of bacteria, T4-like viruses and protists. *ISME J.* 8 (4), 816–829. doi: 10.1038/ismej.2013.199

Couper, L. I., Kwan, J. Y., Ma, J., and Swei, A. (2019). Drivers and patterns of microbial community assembly in a Lyme disease vector. *Ecol. Evol.* 9 (13), 7768–7779. doi: 10.1002/ece3.5361

Crispell, G., Budachetri, K., and Karim, S. (2016). Rickettsia parkeri colonization in amblyomma maculatum: The role of superoxide dismutases. *Parasites Vectors* 9 (1), 291. doi: 10.1186/s13071-016-1579-1

Czech, L., Barbera, P., and Stamatakis, A. (2020). Genesis and gappa: Processing, analyzing and visualizing phylogenetic (placement) data. *Bioinf. (Oxford England)* 36 (10), 3263–3265. doi: 10.1093/bioinformatics/btaa070

Dastgheyb, S. S., and Otto, M. (2015). Staphylococcal adaptation to diverse physiologic niches: An overview of transcriptomic and phenotypic changes in different biological environments. *Future Microbiol.* 10 (12), 1981–1995. doi: 10.2217/fmb.15.116

de la Fuente, J., Antunes, S., Bonnet, S., Cabezas-Cruz, A., Domingos, A. G., Estrada-Peña, A., et al. (2017). Tick-pathogen interactions and vector competence: Identification of molecular drivers for tick-borne diseases. *Front. Cell. infect. Microbiol.* 7. doi: 10.3389/fcimb.2017.00114

de la Fuente, J., Villar, M., Cabezas-Cruz, A., Estrada-Peña, A., Ayllón, N., and Alberdi, P. (2016). Tick-Host-Pathogen interactions: Conflict and cooperation. *PloS Pathog.* 12 (4), e1005488. doi: 10.1371/journal.ppat.1005488

Dhariwal, A., Chong, J., Habib, S., King, I. L., Agellon, L. B., and Xia, J. (2017). Microbiome analyst: A web-based tool for comprehensive statistical, visual and meta-analysis of microbiome data. *Nucleic Acids Res.* 45, (W1) W180–W188. doi: 10.1093/nar/gkx295

Douglas, G. M., Maffei, V. J., Zaneveld, J. R., Yurgel, S. N., Brown, J. R., Taylor, C. M., et al. (2020). PICRUSt2 for prediction of metagenome functions. *Nat. Biotechnol.* 38 (6), 685–688. doi: 10.1038/s41587-020-0548-6

Duron, O., Binetruy, F., Noël, V., Cremaschi, J., McCoy, K. D., Arnathau, C., et al. (2017). Evolutionary changes in symbiont community structure in ticks. *Mol. Ecol.* 26, 2905–2921. doi: 10.1111/mec.14094

Duron, O., Morel, O., Noël, V., Buysse, M., Binetruy, F., Lancelot, R., et al. (2018). Tick-bacteria mutualism depends on b vitamin synthesis pathways. *Curr. biol.: CB* 28 (12), 1896–1902.e5. doi: 10.1016/j.cub.2018.04.038

Duron, O., Noël, V., McCoy, K. D., Bonazzi, M., Sidi-Boumedine, K., Morel, O., et al. (2015). The Recent Evolution of a Maternally-Inherited Endosymbiont of Ticks Led to the Emergence of the Q Fever Pathogen, Coxiella burnetii. *PLoS pathogens*, 11 (5), e1004892. doi: 10.1371/journal.ppat.1004892

Eiler, A., Heinrich, F., and Bertilsson, S. (2012). Coherent dynamics and association networks among lake bacterioplankton taxa. *ISME J.* 6 (2), 330–342. doi: 10.1038/ismej.2011.113

Engel, P., and Moran, N. A. (2013). The gut microbiota of insects – diversity in structure and function. *FEMS Microbiol. Rev.* 37 (5), 699–735. doi: 10.1111/1574-6976.12025

Fiorotti, J., Menna-Barreto, R., Gôlo, P. S., Coutinho-Rodrigues, C., Bitencourt, R., Spadacci-Morena, D. D., et al. (2019). Ultrastructural and cytotoxic effects of metarhizium robertsii infection on rhipicephalus microplus hemocytes. *Front. Physiol.* 10. doi: 10.3389/fphys.2019.00654

Fogaça, A. C., Sousa, G., Pavanelo, D. B., Esteves, E., Martins, L. A., Urbanová, V., et al. (2021). Tick immune system: What is known, the interconnections, the gaps, and the challenges. *Front. Immunol.* 12. doi: 10.3389/fimmu.2021.628054

Franta, Z., Frantová, H., Konvičková, J., Horn, M., Sojka, D., Mareš, M., et al. (2010). Dynamics of digestive proteolytic system during blood feeding of the hard tick ixodes ricinus. *Parasites Vectors* 3, 119. doi: 10.1186/1756-3305-3-119

Friedman, J., and Alm, E. J. (2012). Inferring correlation networks from genomic survey data. *PloS Comput. Biol.* 8 (9), e1002687. doi: 10.1371/journal.pcbi.1002687

Fröhlich, E. (2002). Aufbau und funktion von blut-Gewebe-Schranken [Structure and function of blood-tissue barriers]. *Deutsche medizinische Wochenschrift (1946)* 127 (49), 2629–2634. doi: 10.1055/s-2002-35932

Gaio, A. D. O., Gusmão, D. S., Santos, A. V., Berbert-Molina, M. A., Pimenta, P. F., Lemos, F. J., et al. (2011). Contribution of midgut bacteria to blood digestion and egg production in aedes aegypti (diptera: culicidae) (L.). *Parasites Vectors* 4, 105. doi: 10.1186/1756-3305-4-105

Guizzo, M. G., Budachetri, K., Adegoke, A., Ribeiro, J. M., and Karim, S. (2022) *Rickettsia parkeri* infection modulates the sialome and ovariome of the Gulf coast tick, amblyomma maculatum. *Front. Microbiol.* 13, 1023980. doi: 10.3389/fmicb.2022.1023980

Gil, J. C., Helal, Z. H., Risatti, G., and Hird, S. M. (2020). Ixodes scapularis microbiome correlates with life stage, not the presence of human pathogens, in ticks submitted for diagnostic testing. *PeerJ* 8, e10424. doi: 10.7717/peerj.10424

Gottlieb, Y., Lalzar, I., and Klasson, L. (2015). Distinctive genome reduction rates revealed by genomic analyses of two coxiella-like endosymbionts in ticks. *Genome Biol. Evol.* 7 (6), 1779–1796. doi: 10.1093/gbe/evv108

Greay, T. L., Gofton, A. W., Paparini, A., Ryan, U. M., Oskam, C. L., and Irwin, P. J. (2018). Recent insights into the tick microbiome gained through next-generation sequencing. *Parasites Vectors* 11 (1), 12. doi: 10.1186/s13071-017-2550-5

Guizzo, M. G., Neupane, S., Kucera, M., Perner, J., Frantová, H., da Silva Vaz, I., et al. (2020). Poor unstable midgut microbiome of hard ticks contrasts with abundant and stable monospecific microbiome in ovaries. *Front. Cell. infect. Microbiol.* 10. doi: 10.3389/fcimb.2020.00211

Guizzo, M. G., Parizi, L. F., Nunes, R. D., Schama, R., Albano, R. M., Tirloni, L., et al. (2017). A coxiella mutualist symbiont is essential to the development of rhipicephalus microplus. *Sci. Rep.* 7, 17554. doi: 10.1038/s41598-017-17309-x

Hegde, S., Khanipov, K., Albayrak, L., Golovko, G., Pimenova, M., Saldaña, M. A., et al. (2018). Microbiome Interaction Networks and Community Structure From Laboratory-Reared and Field-Collected Aedes aegypti, Aedes albopictus, and Culex quinquefasciatus Mosquito Vectors. *Frontiers in microbiology* 9, 2160. doi: 10.3389/fmicb.2018.02160

Hillyer, J. F. (2009). Transcription in mosquito hemocytes in response to pathogen exposure. *J. Biol.* 8, 51. doi: 10.1186/jbiol151

Hillyer, J. F., and Strand, M. R. (2014). Mosquito hemocyte-mediated immune responses. *Curr. Opin. Insect Sci.* 3, 14–21. doi: 10.1016/j.cois.2014.07.002

Houk, E. J. (1977). Midgut ultrastructure of culex tarsalis (Diptera: Culcidae) before and after a bloodmeal. *Tissue Cell* 9 (1), 103–118. doi: 10.1016/0040-8166(77)90052-0

Hoxmeier, J. C., Fleshman, A. C., Broeckling, C. D., Prenni, J. E., Dolan, M. C., Gage, K. L., et al. (2017). Metabolomics of the tick-borrelia interaction during the nymphal tick blood meal. *Sci. Rep.* 7, 44394. doi: 10.1038/srep44394

Hunter, D. J., Torkelson, J. L., Bodnar, J., Mortazavi, B., Laurent, T., Deason, J., et al. (2015). The rickettsia endosymbiont of ixodes pacificus contains all the genes of de novo folate biosynthesis. *PloS One* 10 (12), e0144552. doi: 10.1371/journal.pone.0144552

Jing, T. Z., Qi, F. H., and Wang, Z. Y. (2020). Most dominant roles of insect gut bacteria: digestion, detoxification, or essential nutrient provision? *Microbiome* 8, 38. doi: 10.1186/s40168-020-00823

Kadota, K., Walter, S., Claveria, F. G., Igarashi, I., Taylor, D., and Fujisaki, K. (2003). Morphological and populational characteristics of hemocytes of ornithodoros moubata nymphs during the ecdysial phase. *J. Med. Entomol.* 40 (6), 770–776. doi: 10.1603/0022-2585-40.6.770

Karim, S., Budachetri, K., Mukherjee, N., Williams, J., Kausar, A., Hassan, M. J., et al. (2017). A study of ticks and tick-borne livestock pathogens in Pakistan. *PloS Negl. Trop. dis.* 11 (6), e0005681. doi: 10.1371/journal.pntd.0005681

Karim, S., Kumar, D., and Budachetri, K. (2021). Recent advances in understanding tick and rickettsiae interactions. *Parasite immunology* 43 (5), e12830. doi: 10.1111/pim.12830

King, J. G., and Hillyer, J. F. (2013). Spatial and temporal *in vivo* analysis of circulating and sessile immune cells in mosquitoes: Hemocyte mitosis following infection. *BMC Biol.* 11, 55. doi: 10.1186/1741-7007-11-55

Kueneman, J. G., Esser, H. J., Weiss, S. J., Jansen, P. A., and Foley, J. E. (2021). Tick microbiomes in Neotropical forest fragments are best explained by tick-associated and environmental factors rather than host blood source. *Appl. Environ. Microbiol.* 87 (7), e02668–e02620. doi: 10.1128/AEM.02668-20

Kumar, D., Budachetri, K., Meyers, V. C., and Karim, S. (2016). Assessment of tick antioxidant responses to exogenous oxidative stressors and insight into the role of catalase in the reproductive fitness of the gulf coast tick, amblyomma maculatum. *Insect Mol. Biol.* 25 (3), 283–294. doi: 10.1111/imb.12218

Kumar, D., Sharma, S. R., Adegoke, A., Kennedy, A., Tuten, H. C., Li, A. Y., et al. (2022). Recently Evolved Francisella-Like Endosymbiont Outcompetes an Ancient and Evolutionarily Associated Coxiella-Like Endosymbiont in the Lone Star Tick (*Amblyomma americanum*) Linked to the Alpha-Gal Syndrome. *Front. Cell. Infect. Microbiol.* 12, 787209 doi: 10.21203/rs.3.rs-856007/v1

Kurokawa, C., Lynn, G. E., Pedra, J. H. F., Pal, U., Narasimhan, S., Fikrig, E., et al. (2020). Interactions between borrelia burgdorferi and ticks. *Nat. Rev. Microbiol.* 18 (10), 587–600. doi: 10.1038/s41579-020-0400-5

Kwon, H., and Smith, R. C. (2019). Chemical depletion of phagocytic immune cells in anopheles gambiae reveals dual roles of mosquito hemocytes in anti-plasmodium immunity. *Proc. Natl. Acad. Sci. U. S. A.* 116 (28), 14119–14128. doi: 10.1073/pnas.1900147116

Landesman, W. J., Mulder, K., Allan, B. F., Bashor, L. A., Keesing, F., LoGiudice, K., et al. (2019). Potential effects of blood meal host on bacterial community composition in ixodes scapularis nymphs. *Ticks tick-borne Dis.* 10 (3), 523–527. doi: 10.1016/j.ttbdis.2019.01.002

Lejal, E., Moutailler, S., Šimo, L., Vayssier-Taussat, M., and Pollet, T. (2019). Tick-borne pathogen detection in midgut and salivary glands of adult ixodes ricinus. *Parasites Vectors* 12, 152. doi: 10.1186/s13071-019-3418-7

Lejal, E., Chiquet, J., Aubert, J., Robin, S., Estrada-Peña, A., Rue, O., et al. (2021). Temporal patterns in Ixodes ricinus microbial communities: An insight into tick-borne microbe interactions. *Microbiome*, 9 (1), 153. doi: 10.1186/s40168-021-01051-8

Liu, L., Cheng, T. Y., and He, X. M. (2018). Proteomic profiling of the midgut contents of haemaphysalis flava. *Ticks Tick-borne Dis.* 9 (3), 490–495. doi: 10.1016/j.ttbdis.2018.01.008

Liu, L., Narasimhan, S., Dai, J., Zhang, L., Cheng, G., and Fikrig, E. (2011). Ixodes scapularis salivary gland protein P11 facilitates migration of anaplasma

phagocytophilum from the tick gut to salivary glands. *EMBO Rep.* 12 (11), 1196–1203. doi: 10.1038/embor.2011.177

Lopatkin, A. J., and Yang, J. H. (2021). Digital insights into nucleotide metabolism and antibiotic treatment failure. *Front. Digit. Health* 3. doi: 10.3389/fdgth.2021.583468

Louca, S., and Doebeli, M. (2018). Efficient comparative phylogenetics on large trees. *Bioinf. (Oxford England)* 34 (6), 1053–1055. doi: 10.1093/bioinformatics/btx701

Maldonado-Ruiz, L. P., Neupane, S., Park, Y., and Zurek, L. (2021). The bacterial community of the lone star tick (Amblyomma americanum). *Parasites Vectors* 14 (1), 49. doi: 10.1186/s13071-020-04550-z

Mann, A. E., Mitchell, E. A., Zhang, Y., Curtis-Robles, R., Thapa, S., Hamer, S. A., et al. (2020). Comparison of the bacterial gut microbiome of north American triatoma spp. with and without trypanosoma cruzi. *Front. Microbiol.* 11. doi: 10.3389/fmicb.2020.00364

Microsoft Corporation (2018) *Microsoft Excel*. Available at: https://office.microsoft.com/excel.

Mirarab, S., Nguyen, N., and Warnow, T. (2012). SEPP: SATé-enabled phylogenetic placement. pacific symposium on biocomputing. *Pac. Symp. Biocomputing* 2011, 247–258. doi: 10.1142/9789814366496_0024

Mukhacheva, T. A., and Kovalev, S. Y. (2017). Bacteria of the family 'Candidatus midichloriaceae' in sympatric zones of ixodes ticks: Genetic evidence for vertical transmission. *Microbial. Ecol.* 74 (1), 185–193. doi: 10.1007/s00248-017-0932-z

Muturi, E. J., Dunlap, C., Ramirez, J. L., Rooney, A. P., and Kim, C. H. (2019). Host blood-meal source has a strong impact on gut microbiota of *Aedes aegypti*. *FEMS Microbiol. Ecol.* 95 (1), 10.1093/femsec/fiy213. doi: 10.1093/femsec/fiy213

Narasimhan, S., and Fikrig, E. (2015). Tick microbiome: The force within. *Trends Parasitol.* 31 (7), 315–323. doi: 10.1016/j.pt.2015.03.010

Narasimhan, S., Swei, A., Abouneameh, S., Pal, U., Pedra, J., and Fikrig, E. (2021). Grappling with the tick microbiome. *Trends Parasitol.* 37 (8), 722–733. doi: 10.1016/j.pt.2021.04.004

Nuttall, P. A. (2019). Tick saliva and its role in pathogen transmission. *Wiener klinische Wochenschrift* 1, 1–12. doi: 10.1007/s00508-019-1500-y

Nuttall, P., and Labuda, M. (2008). "Saliva-assisted transmission of tick-borne pathogens," in *Ticks: Biology, disease and control*. Eds. A. Bowman and P. Nuttall (Cambridge: Cambridge University Press), 205–219. doi: 10.1017/CBO9780511551802.011

Obregón, D., Bard, E., Abrial, D., Estrada-Peña, A., and Cabezas-Cruz, A. (2019). Sex-specific linkages between taxonomic and functional profiles of tick gut microbiomes. *Front. Cell. infect. Microbiol.* 9. doi: 10.3389/fcimb.2019.00298

Oleaga, A., Obolo-Mvoulouga, P., Manzano-Román, R., and Pérez-Sánchez, R. (2017). A proteomic insight into the midgut proteome of ornithodoros moubata females reveals novel information on blood digestion in argasid ticks. *Parasites Vectors* 10 (1), 366. doi: 10.1186/s13071-017-2300-8

Oliveira, J. L., Cury, J. C., Gurgel-Gonçalves, R., Bahia, A. C., and Monteiro, F. A. (2018). Field-collected triatoma sordida from central Brazil display high microbiota diversity that varies with regard to developmental stage and intestinal segmentation. *PloS Negl. Trop. Dis.* 12 (8), e0006709. doi: 10.1371/journal.pntd.0006709

Olivieri, E., Epis, S., Castelli, M., Varotto Boccazzi, I., Romeo, C., Desirò, A., et al. (2019). Tissue tropism and metabolic pathways of midichloria mitochondrii suggest tissue-specific functions in the symbiosis with ixodes ricinus. *Ticks Tick-Borne Dis.* 10 (5), 1070–1077. doi: 10.1016/j.ttbdis.2019.05.019

Onyango, L. A., and Alreshidi, M. M. (2018). Adaptive metabolism in staphylococci: Survival and persistence in environmental and clinical settings. *J. pathog.* 2018, 1092632. doi: 10.1155/2018/1092632

Paddock, C. D., and Goddard, J. (2015). The evolving medical and veterinary importance of the gulf coast tick (Acari: Ixodidae). *J. Med. Entomol.* 52, 230–252.

Pereira, L. S., Oliveira, P. L., Barja-Fidalgo, C., and Daffre, S. (2001). Production of reactive oxygen species by hemocytes from the cattle tick boophilus microplus. *Exp. Parasitol.* 99 (2), 66–72. doi: 10.1006/expr.2001.4657

Perner, J., Provazník, J., Schrenková, J., Urbanová, V., Ribeiro, J. M., Kopáček, P, et al. (2016). RNA-Seq analyses of the midgut from blood- and serum-fed ixodes ricinus ticks. *Sci. Rep.* 6, 36695. doi: 10.1038/srep36695

Pollet, T., Sprong, H., Lejal, E., Krawczyk, A. I., Moutailler, S., Cosson, J.-F., et al. (2020). The scale affects our view on the identification and distribution of microbial communities in ticks. *Parasit. Vectors* 13 (1), 36. doi: 10.1186/s13071-020-3908-7

Ponnusamy, L., Gonzalez, A., Van Treuren, W., Weiss, S., Parobek, C. M., Juliano, J. J., et al. (2014). Diversity of rickettsiales in the microbiome of the lone star tick, amblyomma americanum. *Appl. Environ. Microbiol.* 80 (1), 354–359. doi: 10.1128/AEM.02987-13

Portillo, A., Palomar, A. M., de Toro, M., Santibáñez, S., Santibáñez, P., and Oteo, J. A. (2019). Exploring the bacteriome in anthropophilic ticks: To investigate the vectors for diagnosis. *PloS One* 14 (3), e0213384. doi: 10.1371/journal.pone.0213384

Powers, J. C., Turangan, R., Joosse, B. A., and Hillyer, J. F. (2020). Adult mosquitoes infected with bacteria early in life have stronger antimicrobial responses and more hemocytes after reinfection later in life. *Insects* 11 (6), 331. doi: 10.3390/insects11060331

Quast, C., Pruesse, E., Yilmaz, P., Gerken, J., Schweer, T., Yarza, P., et al. (2013). The SILVA ribosomal RNA gene database project: Improved data processing and web-based tools. *Nucl. Acids Res.* 41 (D1), D590–D596.

Rachinsky, A., Guerrero, F. D., and Scoles, G. A. (2008). Proteomic profiling of rhipicephalus (Boophilus) microplus midgut responses to infection with babesia bovis. *Vet. Parasitol.* 152 (3-4), 294–313. doi: 10.1016/j.vetpar.2007.12.027

Ravine, T. J. (2019). Bacillus: An environmental contaminant or misunderstood pathogen? *J. Bacteriol. Mycol.* 6 (6), 1117.

Ribeiro, J. M., Zeidner, N. S., Ledin, K., Dolan, M. C., and Mather, T. N. (2004). How much pilocarpine contaminates pilocarpine-induced tick saliva? *Med. Vet. entomol.* 18 (1), 20–24. doi: 10.1111/j.0269-283x.2003.0469

Rojas-Jaimes, J., Lindo-Seminario, D., Correa-Núñez, G., and Diringer, B. (2021). Characterization of the bacterial microbiome of *Rhipicephalus (Boophilus) microplus* collected from pecari tajacu "Sajino" madre de dios, Peru. *Sci. Rep.* 11 (1), 6661. doi: 10.1038/s41598-021-86177-3

Ross, B. D., Hayes, B., Radey, M. C., Lee, X., Josek, T., Bjork, J., et al. (2018). Ixodes scapularis does not harbor a stable midgut microbiome. *ISME J.* 12 (11), 2596–2607. doi: 10.1038/s41396-018-0161-6

Ross, A. A., Rodrigues Hoffmann, A., and Neufeld, J. D. (2019). The skin microbiome of vertebrates. *Microbiome* 7, 79. doi: 10.1186/s40168-019-0694-6

Schwarz, A., Tenzer, S., Hackenberg, M., Erhart, J., Gerhold-Ay, A., Mazur, J., et al. (2014). A systems level analysis reveals transcriptomic and proteomic complexity in ixodes ricinus midgut and salivary glands during early attachment and feeding. *Mol. Cell. Proteomics: MCP* 13 (10), 2725–2735. doi: 10.1074/mcp.M114.039289

Sigle, L. T., and Hillyer, J. F. (2016). Mosquito hemocytes preferentially aggregate and phagocytose pathogens in the periostial regions of the heart that experience the most hemolymph flow. *Dev. Comp. Immunol.* 55, 90–101. doi: 10.1016/j.dci.2015.10.018

Sigle, L. T., and Hillyer, J. F. (2018). Mosquito hemocytes associate with circulatory structures that support intracardiac retrograde hemolymph flow. *Front. Physiol.* 9. doi: 10.3389/fphys.2018.01187

Šimo, L., Kazimirova, M., Richardson, J., and Bonnet, S. I. (2017). The essential role of tick salivary glands and saliva in tick feeding and pathogen transmission. *Front. Cell. Infect. Microbiol.* 7. doi: 10.3389/fcimb.2017.00281

Smith, T. A., Driscoll, T., Gillespie, J. J., and Raghavan, R. (2015). A coxiella-like endosymbiont is a potential vitamin source for the lone star tick. *Genome Biol. Evol.* 7 (3), 831–838. doi: 10.1093/gbe/evv016

Sonenshine, D. E. (2018). Range expansion of tick disease vectors in north America: Implications for spread of tick-borne disease. *Int. J. Environ. Res. Public Health* 15 (3), 478. doi: 10.3390/ijerph15030478

Starck, J. M., Mehnert, L., Biging, A., Bjarsch, J., Franz-Guess, S., Kleeberger, D., et al. (2018). Morphological responses to feeding in ticks (Ixodes ricinus). *Zool. Lett.* 4, 20. doi: 10.1186/s40851-018-0104-0

Swei, A., and Kwan, J. (2017). Tick microbiome and pathogen acquisition altered by host blood meal. *ISME J.* 11, 813–816. doi: 10.1038/ismej.2016.152

Tarnowski, B. I., and Coons, L. B. (1989). Ultrastructure of the midgut and blood meal digestion in the adult tick dermacentor variabilis. *Exp. Appl. acarol.* 6 (4), 263–289. doi: 10.1007/BF01193300

Thapa, S., Zhang, Y., and Allen, M. S. (2019a). Bacterial microbiomes of ixodes scapularis ticks collected from Massachusetts and Texas, USA. *BMC Microbiol.* 19, 138. doi: 10.1186/s12866-019-1514-7

Thapa, S., Zhang, Y., and Allen, M. S. (2019b). Effects of temperature on bacterial microbiome composition in ixodes scapularis ticks. *MicrobiologyOpen* 8 (5), e00719. doi: 10.1002/mbo3.719

Tirloni, L., Braz, G., Nunes, R. D., Gandara, A., Vieira, L. R., Assumpcao, T. C., et al. (2020). A physiologic overview of the organ-specific transcriptome of the cattle tick rhipicephalus microplus. *Sci. Rep.* 10, 18296. doi: 10.1038/s41598-020-75341-w

Trappeniers, K., Matetovici, I., Van Den Abbeele, J., and De Vooght, L. (2019). The tsetse fly displays an attenuated immune response to its secondary symbiont, sodalis glossinidius. *Front. Microbiol.* 10. doi: 10.3389/fmicb.2019.01650

Trout Fryxell, R. T., and DeBruyn, J. M. (2016). The microbiome of ehrlichia-infected and uninfected lone star ticks (Amblyomma americanum). *PloS One* 11 (1), e0146651. doi: 10.1371/journal.pone.0146651

Valenzuela, J. G., Charlab, R., Mather, T. N., and Ribeiro, J. M. (2000). Purification, cloning, and expression of a novel salivary anticomplement protein from the tick, ixodes scapularis. *J. Biol. Chem.* 275 (25), 18717–18723. doi: 10.1074/jbc.M001486200

Varela-Stokes, A. S., Park, S. H., Stokes, J. V., Gavron, N. A., Lee, S. I., Moraru, G. M., et al. (2018). Tick microbial communities within enriched extracts of amblyomma maculatum. *Ticks Tick-borne Dis.* 9 (4), 798–805. doi: 10.1016/j.ttbdis.2018.02.022

Wei, N., Cao, J., Zhang, H., Zhou, Y., and Zhou, J. (2021). The tick microbiota dysbiosis promote tick-borne pathogen transstadial transmission in a babesia microti-infected mouse model. *Front. Cell. Infect. Microbiol.* 11. doi: 10.3389/fcimb.2021.713466

Wright, C. L., Gaff, H. D., Sonenshine, D. E., and Hynes, W. L. (2015). Experimental vertical transmission of rickettsia parkeri in the gulf coast tick, amblyomma maculatum. *Ticks Tick-borne Dis.* 6 (5), 568–573. doi: 10.1016/j.ttbdis.2015.04.011

Wu-Chuang, A., Hodžić, A., Mateos-Hernández, L., Estrada-Peña, A., Obregon, D., and Cabezas-Cruz, A. (2021). Current debates and advances in tick microbiome research. *Curr. Res. Parasitol. Vector-borne Dis.* 1, 100036. doi: 10.1016/j.crpvbd.2021.100036

Ye, Y., and Doak, T. G. (2009). A parsimony approach to biological pathway reconstruction/inference for genomes and metagenomes. *PloS Comput. Biol.* 5 (8), e1000465. doi: 10.1371/journal.pcbi.1000465

Zhang, X. C., Yang, Z. N., Lu, B., Ma, X. F., Zhang, C. X., and Xu, H. J. (2014). The composition and transmission of microbiome in hard tick, ixodes persulcatus, during blood meal. *Ticks Tick-borne Dis.* 5 (6), 864–870. doi: 10.1016/j.ttbdis.2014.07.009

Zhang, Y. K., Yu, Z. J., Wang, D., Bronislava, V., Branislav, P., Liu, J. Z., et al. (2019). The bacterial microbiome of field-collected dermacentor marginatus and dermacentor reticulatus from Slovakia. *Parasites Vectors* 12 (1), 325. doi: 10.1186/s13071-019-3582-9

Zhong, J., Jasinskas, A., and Barbour, A. G. (2007). Antibiotic treatment of the tick vector amblyomma americanum reduced reproductive fitness. *PloS One* 2 (5), e405. doi: 10.1371/journal.pone.0000405

Zolnik, C. P., Falco, R. C., Daniels, T. J., and Kolokotronis, S. O. (2018). Transient influence of blood meal and natural environment on blacklegged tick bacterial communities. *Ticks Tick-borne Dis.* 9 (3), 563–572. doi: 10.1016/j.ttbdis.2018.01.007

Zolnik, C. P., Prill, R. J., Falco, R. C., Daniels, T. J., and Kolokotronis, S. O. (2016). Microbiome changes through ontogeny of a tick pathogen vector. *Mol. Ecol.* 25 (19), 4963–4977. doi: 10.1111/mec.13832